AFRL-HE-WP-TR-2007-0084

Development and Validation of ATB Model for THOR-NT Dummy

Tariq Shams

GESAC, Inc.
125 Orchard Drive
Boonsboro MD 21713

Huaining Cheng
Joseph A. Pellettiere

Biosciences and Protection Division
Biomechanics Branch

May 2007
Final Report for August 2005 to May 2007

Air Force Research Laboratory
Human Effectiveness Directorate
Biosciences and Protection Division
Biomechanics Branch
Wright-Patterson AFB OH 45433-7947

NOTICE AND SIGNATURE PAGE

AFRL-HE-WP-TR-2007-0084

//SIGNED//	//SIGNED//
NATHAN WRIGHT, Work Unit Manager Biomechanics Branch	MARK M. HOFFMAN Biosciences & Protection Division Human Effectiveness Directorate Air Force Research Laboratory

REPORT DOCUMENTATION PAGE

Form Approved
OMB No. 074-0188

PLEASE DO NOT RETURN YOUR FORM TO THE ABOVE ADDRESS.

1. REPORT DATE (DD-MMM-YYYY)	2. REPORT TYPE	3. DATES COVERED (From – To)
May 2007	Final Report	August 2005 to May 2007

4. TITLE AND SUBTITLE

Development and Validation of ATB Model for THOR-NT Dummy

5a. CONTRACT NUMBER
FA8650-04-D-6472

5b. GRANT NUMBER

5c. PROGRAM ELEMENT NUMBER
62202F

6. AUTHOR(S)

Tariq Shams*
Huaining Cheng **
Joseph A. Pellettiere **

5d. PROJECT NUMBER
7184

5e. TASK NUMBER
02

5f. WORKUNIT NUMBER
11

7. PERFORMING ORGANIZATION NAME(S) AND ADDRESS(ES)

*GESAC, Inc.
125 Orchard Drive
Boonsboro MD 21713

8. PERFORMING ORGANIZATION REPORT NUMBER

9. SPONSORING / MONITORING AGENCY NAME(S) AND ADDRESS(ES)

Air Force Materiel Command **
Air Force Research Laboratory
Human Effectiveness Directorate
Biosciences & Protection Division
Biomechanics Branch
Wright-Patterson AFB OH 45433-7947

10. SPONSOR / MONITOR'S ACRONYM

AFRL/HEPA

11. SPONSOR/MONITOR'S REPORT NUMBER(S)

AFRL-HE-WP-TR-2007-0084

12. DISTRIBUTION / AVAILABILITY STATEMENT

Approved for public release; distribution is unlimited.

13. SUPPLEMENTARY NOTES

Cleared by AFRL/PA as AFRL/WS-07-1794 on 6 Aug 07.

14. ABSTRACT

THOR-NT is the National Highway Traffic Safety Administration's (NHTSA) Advanced Frontal Impact Dummy. GESAC, Inc., in cooperation with NHTSA and Air Force Research Laboratory (AFRL), has developed the Articulated Total Body (ATB) model for the THOR-NT dummy. ATB is a rigid-body dynamics simulation program. The ATB THOR-NT model consists of 21 segments coupled by 20 joints. Segment mass properties, joint mechanical properties, and surface contact properties were modeled from test data collected through quasi-static and dynamic tests. A set of ATB simulations were developed for the THOR-NT certification tests. The results were compared and analyzed. The simulations reproduced the test responses reasonably well. This work demonstrated that ATB model can serve as an effective preliminary assessment tool for studies involving THOR-NT dummy.

15. SUBJECT TERMS

Manikins, Crash Simulation, Biodynamic Response, Impact Test

16. SECURITY CLASSIFICATION OF:			17. LIMITATION OF ABSTRACT	18. NUMBER OF PAGES	19a. NAME OF RESPONSIBLE PERSON:
a. REPORT	b. ABSTRACT	c. THIS PAGE			Huaining Cheng
U	U	U	SAR	89	19b. TELEPHONE NUMBER *(Include area code)*

THIS PAGE IS INTENTIONALLY LEFT BLANK

TABLE OF CONTENTS

LIST OF FIGURES

LIST OF TABLES

PREFACE

This report documents the development and validation of ATB Model for THOR-NT dummy. The work was conducted by Dr. Tariq Shams of General Engineering and Systems Analysis Company, Inc. (GESAC) under a subcontract to General Dynamics Corp. It was a collaborative effort among National Highway Traffic Safety Administration (NHTSA), Air Force Research Laboratory (AFRL), and GESAC. Dr. Joseph A. Pellettiere of AFRL was the technical monitor for the work and Mr. Eric Ennis of AFRL modified GEBOD program for the addition of THOR-NT dataset.

THIS PAGE IS INTENTIONALLY LEFT BLANK

1. INTRODUCTION

The improved version of NHTSA's (National Highway Traffic Safety Administration) Advanced Frontal Impact Dummy, THOR-NT (GESAC, 2005) has been undergoing tests and validations. Compared to the previous generations of dummies, THOR-NT incorporates enhanced anthropometry, biofidelity, and instrumentation. One part of these validation efforts was to develop an ATB model for the THOR-NT dummy and validate it against component tests and full body sled tests. This report summarizes the work done by the GESAC Inc. on the THOR-NT ATB model development and validation as well as the addition of THOR-NT data set into the GEBOD program (Gross, 1991; Cheng, Obergefell, & Rizer, 1994).

ATB (Articulated Total Body Model) (Obergefell, Kaleps, Gardner, & Fleck, 1988; Cheng, Rizer, & Obergefell, 1998) is a coupled rigid body dynamics simulation program originated from the CVS (Crash Victim Simulator) program developed at the Calspan Corporation (Fleck & Butler, 1982). The latest version is version V.3-1 (Gardner, 2004). It models a human body or dummy in multiple segments articulated by angular and linear joints. Each segment has mass, principal moments of inertia, and orientation of principal axes defined with respect to a local reference system that is attached to the segment's center of mass. The volume shape of the segment is represented by a contact ellipsoid attached to the segment's local reference system. The ellipsoid's size is derived from the anthropometric measurements of the corresponding human body or dummy segment. Occasionally, more than one contact ellipsoid can be attached to a particular segment to offer a better representation of its actual shape. The joint that connects two adjacent segments is defined through two joint coordinate systems which have the same origin but attach to each of the segments respectively. The types of joints modeled by the ATB program include pin, ball, socket, free, Euler, and slip joints. The joint mechanical properties consist of joint range of free motion and joint resistive torques which regulate joint angles and velocities.

Existing ATB dummy models use either 17 segments coupled by 16 joints (Hybrid III) or 15 segments coupled by 14 joints (Hybrid II). THOR-NT is more complex than both and is modeled using 21 segments coupled by 20 joints.

The dynamic environment for an ATB simulation is modeled mostly by a set of contact planes. These planes are parallelograms that can form a vehicle compartment, aircraft cockpit, or wheel chair etc. They do not have any inertial properties and only provide contact surface. They are attached to a vehicle segment which usually has a prescribed motion. This in turn creates a dynamic environment in which contacts among segments' contact ellipsoids as well as between contact ellipsoids and planes can be modeled.

The contact forces are proportional to the penetrations between ellipsoids and ellipsoids or ellipsoids and planes. They are computed according to contact functions which set the relationships between penetrations and resulting contact forces. The relationships can consist of force-deflection, inertial spike, energy absorption, permanent deflection, friction, and rate-dependent viscous effects.

The ATB program also has the capability of modeling certain common restraint systems. These include spring-dampers between two segments, external forces and torques on a segment, and harness belt systems over multiple segments. A harness is made up of one or several interactive belts that cross over a set of reference points that are defined on the surface of the restrained segments. The end reference points are either anchor points fixed to vehicle segments or tie points with other belts. The reference points are points of contact between the belts and segments' contact ellipsoids. They can penetrate into and slide over the surface of the contact ellipsoids and as such create the interaction between the belts and

the segments. The contact and friction forces between belts and ellipsoids are computed in a similar way as other contact forces. The belt forces are calculated according to strain or strain-rate-dependent belt force functions.

The above data, together with initial conditions and simulation control parameters, are typical input data to ATB simulations. Figure 1 shows a sample configuration of ATB simulations.

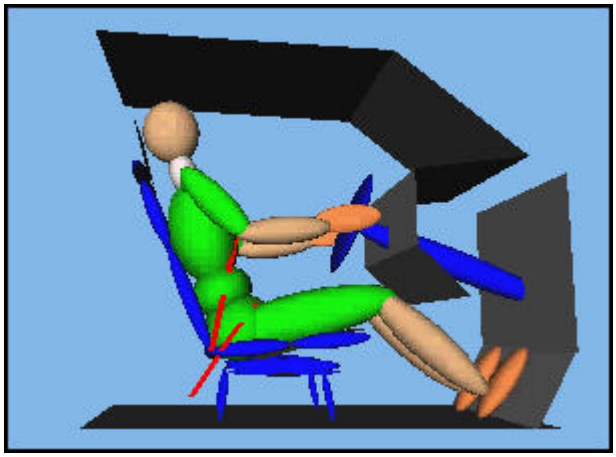

Figure 1: One Frame View of a Typical ATB Simulation

The results from an ATB simulation consist of time histories of kinematic and dynamic data and graphical data for the creation of 3-D animation. The main time histories are:

1. Segment linear and angular accelerations, velocities, and positions
2. Joint angles, forces, and resistive torques
3. Contact forces and deflections between ellipsoids/ellipsoids, ellipsoids/planes, and ellipsoids/belts
4. Other forces such as spring-dampers and external forces/torques

These output data can be used against test data to validate model or perform injury assessment. In this project, GESAC developed ATB models for full body THOR-NT dummy as well as various dummy components used for certification tests. The time histories from ATB simulations of these models were compared with certification tests to validate the ATB model of THOR-NT dummy.

A portion of the development work was directly based on or modified from data sets of DYNAMAN program whose numerical solver was modified from ATB version IV. Because of the progress of both programs, they may have some small differences in simulation results.

2. ATB MODEL OF THOR-NT DUMMY

Like other traditional dummies, the THOR-NT dummy consists of a number of segments that are joined together at well defined joints with varying degrees of freedom. The ATB data set of the dummy consists of segments, joints, and joint resistive torque functions. They form the ATB input cards B and E. They are described in the following sections.

2.1. THOR-NT Dummy Summary

The THOR-NT has a number of special features, which are distinct from the Hybrid III dummy. There are more deformable components within the dummy which require more segments as part of the dummy definition. A brief description of THOR-NT is given below.

Head/Face: It has a deformable and instrumented face. The face is biofidelic under normal impact loads, and can measure loads at five locations. It also contains the mounting platform for placing a nine accelerometer package for measuring angular accelerations.

Neck: The neck is biofidelic in frontal and lateral flexion. There are spring/cable systems in front and rear to model musculature, and there is an occipital condyle joint (OC) which allows continuously increasing resistance in extension and frontal flexion. 6-axis upper and lower neck load cells can be attached to measure neck loads.

Shoulder: The shoulder joint allows for several movements. There is the normal movement of the upper arm relative to the shoulder through a universal joint allowing for flexion/extension and abduction/adduction. There is also a fore/aft movement of the main shoulder assembly about the spine and a more restrictive movement of the clavicles with respect to the sternum and the shoulder.

Spine: There is an additional flexible joint within thoracic spine (approximately at T7/T8), in addition to flexible lumbar spine. Triaxial accelerometers can be placed at the top, mid, and bottom of the thoracic spine.

Thorax: Ribcage with seven slanted, elliptically shaped ribs has been designed to meet standard Kroell corridors for sternal impact at 4.3 m/s and 6.7 m/s and oblique lower cage impact at 4.3 m/s. 3-D deflections can be measured at four locations on the anterior portion of the ribcage using a linkage system called the CRUX.

Abdomen: Both upper and lower abdomen meet biofidelity corridors for impact with steering wheel rim and straight rod respectively. A string pot is used to measure deflections of the upper abdomen, and a pair of double-gimballed string potentiometers (DGSPs) can measure 3-D deflections at two locations on the midline of the lower abdomen.

Pelvis: An anthropometric pelvis (with proper representation of the anterior superior iliac spine, ischial tuberosities, and posterior superior iliac spine) has 3-axis load cells to measure loads on the left and right acetabula.

Femur: The femur contains a deformable component (under axial loading) to make knee impacts more biofidelic. The standard Hybrid III femur load cell can be inserted into the THOR femur.

Tibia: The tibia contains a deformable component (under axial loading) to make plantar impacts more biofidelic. Loads on the tibia are measured with 4-axis load cells at the above and below the deformable component.

Ankle: Full 3 DOF motion is allowed through individual pin joints. The ankle response is biofidelic in dynamic dorsiflexion/plantarflexion and quasi-static inversion/eversion and external/internal rotations. A biofidelic representation of the Achilles' tendon (under dorsiflexion/plantarflexion) is also part of the tibia/ankle assembly. Rotations in all three directions are measured with rotary potentiometers.

Foot: The foot consists of a carbon fiber foot plate with flesh and a heel pad to provide biofidelic response in a heel impact (in conjunction with the tibia puck). A triaxial accelerometer can be placed to measure foot accelerations.

2.2. Segmentation and Inertial and Geometry Properties

GESAC has a torsional pendulum (trifilar) that was used to measure both C.G. (center of gravity) along anatomical (or structural) axes and the moments of inertia about these axes. A V-block was used to rotate the structure for measuring intermediate directions (for measurement of product moments of inertia). GESAC has measured the inertial properties of the components of the previous iteration of the THOR dummy known as THOR-Alpha and used those for the THOR-NT because they have the same segmentation. The contact ellipsoid definitions were made from the CAD drawings for the individual segments or their nearest equivalents.

2.2.1. Segment Mass Properties

The mass, center of gravity, and moment of inertia data (Table 1) for the THOR-NT segments were measured (note the Hybrid III 50th percentile male upper and lower arms are retained in the THOR design and their inertia data remain unchanged). The C.G. is measured from selected skeletal landmarks for each segment in their individual segment coordinate systems. The axes system is in accordance with the standard SAE J1733 conventions. In the convention, for each segment, the X axis is in the posterior anterior direction, the Y axis in the medial-lateral, and the Z axis in the superior-inferior (when the body is standing erect). The C.G. and MOI (moment of inertia) are presented along the X, Y, and Z axes. The rotation angles are for the principal axis directions are in the yaw, pitch, and roll order (Y, P, R). These data were used to form the B.1 and B.2 cards in the ATB input file.

Table 1. THOR-NT Segment Mass, C.G., and Moment of Inertia
(in English units: mass = lbs, length = in., MOI = lb-in-sec^2)

Segment	Mass	C.G. (X, Y, Z)	MOI (X, Y, Z)	Angles (Y, P, R)
Head	10.16	1.70	0.187	0
		1.07	0.203	37
		-1.71	0.131	0
Neck	3.64	-1.02	0.043	0
		1.03	0.043	0
		2.13	0.007	0
Upper Thorax	29.59	0.08	1.295	0
		-0.04	0.631	-25
		1.12	1.414	0
Lower Thorax	21.91	3.33	0.604	0
		1.08	0.589	0
		6.92	0.483	0
Pelvis	33.60	1.91	1.286	0
		1.13	0.948	45
		2.92	0.890	0
Right Upper Femur	6.77	0.77	0.144	0
		1.87	0.123	0
		-0.05	0.048	0
Right Lower Femur	9.81	-0.66	0.267	0
		-1.19	0.291	0
		7.27	0.077	0
Right Upper Tibia	3.97	0.42	0.070	0
		0.24	0.069	0
		1.31	0.015	0
Right Lower Tibia	4.41	0.65	0.092	0
		0.93	0.097	0
		-4.29	0.015	0

Segment	Mass	C.G. (X, Y, Z)	MOI (X, Y, Z)	Angles (Y, P, R)
Right Foot	2.09	1.84	0.024	-161
		0.70	0.047	6
		0.42	0.046	15
Left Upper Femur	6.77	0.77	0.144	0
		1.87	0.123	0
		-0.05	0.048	0
Left Lower Femur	9.81	-0.66	0.267	0
		-1.19	0.291	0
		7.27	0.077	0
Left Upper Tibia	3.97	0.42	0.070	0
		0.24	0.069	0
		1.31	0.015	0
Left Lower Tibia	4.41	0.65	0.092	0
		0.93	0.097	0
		-4.29	0.015	0
Left Foot	2.09	1.84	0.024	161
		0.70	0.047	-6
		0.42	0.046	-15

Note: (i) For the upper and lower thorax segments, small off-axis components were normally zeroed out to ensure sagittal symmetry.
(ii) The accuracy of the MOI measurement system is approximately .001 lb-in-sec^2. Product MOI components smaller than this were zeroed out.
(iii) For obtaining the yaw, pitch, and roll angles from the direction cosine matrix of the MOI principal axes, components smaller than .05 were zeroed out.
(iv) The C.G. distance measurements have been rounded to .01 in.

Description of Segment Origin and Coordinate Systems

Head:	Origin	Center of O.C. joint
	Coordinate System	Aligned with bottom skull plate
Neck:	Origin	Center of O.C. joint
	Coordinate System	Aligned with upper neck load cell
Upper Thorax:	Origin	Center of upper surface of lower neck load cell
	Coordinate System	Aligned with lower neck load cell

Lower Thorax:	Origin	Center of top of lower thoracic spine welded assembly
	Coordinate System	Aligned with lower thoracic spine
Pelvis:	Origin	Center of pelvis/lumbar adapter block
	Coordinate System	Aligned with pelvis/lumbar adapter block
Upper Femur:	Origin	Center of distal surface of hip cylinder
	Coordinate System	Aligned with center line through hip cylinder
Lower Femur:	Origin	Center of distal end cap of femur compliant bushing
	Coordinate System	Aligned with center line through knee housing
Upper Tibia:	Origin	Center of bottom of knee clevis assembly
	Coordinate System	Aligned with center line through upper tibia load cell
Lower Tibia:	Origin	Center of ankle joint
	Coordinate System	Aligned with center line through tibia tube
Foot:	Origin	Center of ankle joint
	Coordinate System	Aligned with screw holes for attaching ankle assembly

Among the segments, the head has a deformable face; its properties are included as part of the force deflection function of the front of the head (using an additional ellipsoid). This additional ellipsoid data is included in the ATB input file as one of the D.5 cards and the force deflection function for the deformable face is include as one of the E.1 to E.4 cards. The THOR-NT neck consists of five rubber disks with a front and rear spring/cable assembly which mimics the action of the neck muscles, and an OC joint with continuous moment resistance in frontal flexion and extension. During the THOR-NT design phase, GESAC developed a spring/damper model to model each of the five rubber disks in the neck. Each disk is modeled with a pair of spring/dampers - one in front and one in rear. The model is geared for motion in one-plane, i.e. either sagittal (flexion/extension) or lateral, and the model appeared to work well for in-plane motions. One set of 10 spring/dampers for flexion/extension and another set for lateral only were used for specific types of tests. However, this modeling approach is not practical to use in a general model where the neck can move in any direction and at least 20 spring/dampers would have to be used. Therefore the model was revised back to one rigid neck with two joints. The shoulder assembly is a relatively complicated structure. The rear component of the shoulder is defined as a separate segment since there is a well-defined fore-aft rotation about the spine. This segment would then connect at the upper arm joint to the arm segment. Though there are separate clavicles, the movement of the clavicles is small. Thus their influence is represented through additional ellipsoids for representing belt contacts. This additional ellipsoid is included in the ATB input file as another D.5 card. The torso is divided into upper thorax, lower thorax, and pelvis connected by two joints. The upper leg or femur contains a compressible element that divides the upper leg into two segments. Thus there are two inertial segments defining the upper leg connected by a slip joint, which allows only axial movement. The lower leg or tibia also contains a compressible element that divides the leg into two segments. Thus there are two inertial segments defining the lower leg connected by a slip joint allowing only axial movement.

2.2.2. Segment Contact Ellipsoid Data

The ellipsoid semiaxes and the location of the center with respect to the C.G. of the corresponding segment for each of the THOR-NT segments were calculated from drawings (Table 2).

Table 2. Segment Contact Ellipsoid Data (measurements are in inches)

Segment	**Semiaxis X**	**Semiaxis Y**	**Semiaxis Z**	**Center X**	**Center Y**	**Center Z**
Head	4.0	3.125	4.5	-0.4	0.0	0.0
Neck	1.5	1.5	2.5	0.0	0.0	0.8
Upper Thorax	4.375	5.5	7.0	0.5	0.0	2.4
Lower Thorax	4.75	6.0	8.0	0.0	0.0	3.2
Pelvis	5.0	7.5	5.0	0.7	0.0	-1.5
Right Upper Femur	3.5	3.5	7.0	-0.3	-0.5	0.5
Right Lower Femur	4.0	3.25	9.5	0.0	0.0	-4.4
Right Upper Tibia	2.25	2.25	6.5	-2.0	-1.1	-0.3
Right Lower Tibia	2.25	1.75	10.0	0.7	0.0	3.0
Right Foot	5.5	1.75	1.5	0.7	0.0	0.3
Left Upper Femur	3.5	3.5	7.0	-0.3	0.5	0.5
Left Lower Femur	4.0	3.25	9.5	0.0	0.0	-4.4
Left Upper Tibia	2.25	2.25	6.5	-2.0	1.1	-0.3
Left Lower Tibia	2.25	1.75	10.0	0.7	0.0	3.0
Right Foot	5.5	1.75	1.5	0.7	0.0	0.3

Note: (i) The locations of the centers of the ellipsoids have been approximated to either 1/8 in or 0.1 in as appropriate.

2.3. Joints Data of ATB THOR-NT Model

The joints are defined based on the segments (Table 2). The joint locations with respect to previous and next segments and joint axes directions relative to segment principal axes are measured using the CAD drawings. The joint characteristics are developed from existing joint response data. Quasi-static tests and dynamic tests have been performed on most of the joints in the THOR-NT. These provide moment vs. angle data for both loading and unloading as well as amount of hysteresis (and effective residual deformation). The standard joints at the shoulder, hip, neck, and spine and ankle are defined through a set of joint functions that depend on two joint angles, flexure and azimuth. The compressible elements which are specific to the THOR in the femur and tibia were represented as slip joints and defined using the spring functions. The following joint data were used to form ATB input cards of B.3 to B.5 as well as input cards E.7.

2.3.1. Joint Type, Location, and Orientation

Joint locations were obtained from the 3-D CAD drawings of the individual segments after determination of the segment C.G. and the local axes system. The joint type and location with respect to the segment origin in segment local coordinate system was defined for each joint (Table 3)

Table 3. Joint Type and Location (measurement are in inches)

Joint	**Type**	**Segment**	**X**	**Y**	**Z**
Lumbar Flx Jt	Free; Defined by joint function	Pelvis	-1.54	0.0	-4.42
		Lower Thorax	-1.30	0.0	2.35
Thoracic Flx Jt	Free; Defined by joint function	Lower Thorax	-1.90	0.0	-6.9
		Upper Thorax	-1.45	0.0	3.25
Neck Bottom	Free; Defined by joint function	Upper Thorax	-0.85	0.0	-1.43
		Neck	0.10	0.0	4.00
O.C.	Free; Defined by joint function	Neck	0.1	0.0	-2.63
		Head	-0.64	0.0	1.96
R. Hip Jt	Free; Defined by joint function	Pelvis	0.95	3.29	1.50
		R. Up Femur	0.0	-1.20	-3.50
R. Femur Jt	Slip; Defined by spring function	R. Up Femur	-0.1	0.2	2.80
		R. Lo Femur	0.3	-0.1	-7.25

Joint	Type	Segment	X	Y	Z
R. Knee	Pin; Std H3	R. Lo Femur	0.3	-0.1	2.70
		R. Up Tibia	0.0	-0.15	-4.20
R. Tibia Jt	Slip; Defined by spring function	R. Up Tibia	-0.1	0.0	2.80
		R. Lo Tibia	0.0	0.15	-5.30
R. Ankle	Free; Defined by joint function	R. Lo Tibia	0.1	0.15	4.70
		R. Foot	-1.10	0.0	-1.45
L. Hip Jt	Free; Defined by joint function	Pelvis	0.95	-3.29	1.50
		L. Up Femur	0.0	1.20	-3.50
L. Femur Jt	Slip; defined by spring function	L. Up Femur	-0.1	-0.2	2.80
		L. Lo Femur	0.3	0.1	-7.25
L. Knee	Pin; Std H3	L. Lo Femur	0.3	0.1	2.70
		L. Up Tibia	0.0	0.15	-4.20
L. Tibia Jt	Slip; Defined by spring function	L. Up Tibia	-0.1	0.00	2.80
		L. Lo Tibia	0.0	-0.15	-5.30
L. Ankle	Free; Defined by joint function	L. Lo Tibia	0.1	-0.15	4.70
		L. Foot	-1.1	0.0	-1.45
R. Shoulder	Free; Defined by joint function	Upper Thorax	-0.88	7.38	-2.66
L. Shoulder	Free; Defined by joint function	Upper Thorax	-0.88	-7.38	-2.66

Note: Hybrid III arms are used in THOR-NT, and all joint locations wrt upper arm, lower arm, and hand remain the same.

The joint orientation data are similar to the Hybrid III; for the shoulder and hip joints, the joint axes for the previous segment are rotated in pitch by 90 degrees. The ankle joint orientation has been revised,

since the joint is now defined using joint functions for the ankle. Joint orientations with respect to the segment local reference system were defined (Table 4).

Table 4. Joint Orientation (measurements are in degrees)

Joint	Segment	Yaw	Pitch	Roll
Lumbar Flx Jt	Pelvis	0.0	0.0	0.0
	Lower Thorax	0.0	0.0	0.0
Thoracic Flx Jt	Lower Thorax	0.0	0.0	0.0
	Upper Thorax	0.0	0.0	0.0
Neck Bottom	Upper Thorax	0.0	0.0	0.0
	Neck	0.0	0.0	0.0
O.C.	Neck	0.0	0.0	0.0
	Head	0.0	0.0	0.0
R. Hip Jt	Pelvis	0.0	90.0	0.0
	R. Up Femur	0.0	0.0	0.0
R. Femur Jt	R. Up Femur	0.0	0.0	0.0
	R. Lo Femur	0.0	0.0	0.0
R. Knee	R. Lo Femur	0.0	0.0	0.0
	R. Up Tibia	0.0	55.0	0.0
R. Tibia Jt	R. Up Tibia	0.0	0.0	0.0
	R. Lo Tibia	0.0	0.0	0.0
R. Ankle	R. Lo Tibia	0.0	0.0	0.0
	R. Foot	0.0	0.0	0.0
L. Hip Jt	Pelvis	0.0	90.0	0.0
	L. Up Femur	0.0	0.0	0.0
L. Femur Jt	L. Up Femur	0.0	0.0	0.0
	L. Lo Femur	0.0	0.0	0.0
L. Knee	L. Lo Femur	0.0	0.0	0.0
	L. Up Tibia	0.0	55.0	0.0
L. Tibia Jt	L. Up Tibia	0.0	0.0	0.0
	L. Lo Tibia	0.0	0.0	0.0

Joint	Segment	Yaw	Pitch	Roll
L. Ankle	L. Lo Tibia	0.0	0.0	0.0
	L. Foot	0.0	0.0	0.0
R. Shoulder	Upper Thorax	0.0	90.0	0.0
L. Shoulder	Upper Thorax	0.0	90.0	0.0

2.3.2. Joint Resistive Torque Functions

The joint functions were obtained from quasi-static bending tests of the joints, generally in four perpendicular directions. The function values for the full range of 180 degrees were obtained by extrapolation.

Hip

Measurements were made for four rotations - flexion, extension, abduction, and adduction. It was difficult to fit a polynomial to the data, so it was kept in tabular form. Also, as the data did vary during the first 30 degrees or so, it was necessary to keep the angle interval at 10 degrees (Table 5).

Table 5. Hip Joint Properties

Joint Angle (deg)	Extension Torque (in-lbs)	Adduction Torque (in-lbs)	Flexion Torque (in-lbs)	Abduction Torque (in-lbs)
0	0	0	0	0
10	80	130	150	50
20	180	440	180	90
30	280	930	230	540
40	390	1600	280	600
50	490	2500	350	790
60	610	3500	430	1100
70	720	4800	530	1500
80	830	6200	660	2100
90	950	7800	810	2800
100	1100	9500	1000	3600
110	1200	12000	1200	4500
120	1300	14000	1500	5500
130	1400	16000	1900	6700
140	1600	19000	2400	8000
150	1700	21000	2900	9400
160	1800	24000	3600	11000
170	2000	27000	4500	13000
180	2100	30000	5600	14000

The values for the left hip joint were obtained by reflecting about the ZX plane, by switching the tables for abduction and adduction.

Shoulder

It was possible to fit a quadratic curve to the shoulder joint data (Table 6). Data were obtained from rotations in four directions (extension, adduction, flexion, adduction).

Table 6. Shoulder Joint Properties

Direction	**Dead Band (deg)**	**Coeff 1 (in-lbs/rad)**	**Coeff 2 (in-lbs/rad^2)**
Extension	165.0000	-520.0000	5320.000
Adduction	0.000000	150.0000	240.0000
Flexion	30.00000	0.000000	310.0000
Abduction	115.0000	210.0000	380.0000

The values for the left shoulder were obtained by reflecting about the ZX plane.

Lumbar Joint

The data for the lumbar joint indicated a linear fit would be satisfactory for the range of motion expected. The joint is not expected to produce bending greater than 40 degrees during most normal testing. Since the extrapolation to higher range was hypothetical, a simple linear fit was considered satisfactory (Table 7).

Table 7. Lumbar Joint Properties

Direction	**Dead Band (deg)**	**Coeff 1 (in-lbs/rad)**
Extension	0.000000	2660.000
Adduction	0.000000	7140.000
Flexion	0.000000	2660.000
Abuction	0.000000	7140.000

Thoracic Joint

The data for the thoracic flex joint was similar to the lumbar joint, and a linear fit was considered satisfactory (Table 8).

Table 8. Thoracic Joint Properties

Direction	**Dead Band (deg)**	**Coeff 1 (in-lbs/rad)**
Extension	0.000000	4930.000
Adduction	0.000000	21400.00
Flexion	0.000000	4930.000
Abuction	0.000000	21400.00

Neck Bottom

The moment-angle characteristic of the neck column was distributed equally to the top and the bottom of the neck, similar to that done for the Hybrid III neck (Table 9). One change was the combination of O.C. joint in the THOR neck with the moment-angle characteristic at the top of the neck. Since THOR allows a fair amount of rotation (about the Y-axis) in flexion and extension at the O.C., this reduced the moments generated (for the same angles) at the top compared to the bottom of the neck.

Table 9. Neck Bottom Joint Properties

Joint Angle (deg)	Extension Torque (in-lbs)	Adduction Torque (in-lbs)	Flexion Torque (in-lbs)	Abduction Torque (in-lbs)
0	0.000000	0.000000	0.000000	0.000000
20	800.0000	1120.000	710.0000	1120.000
40	1400.000	1500.000	989.9999	1500.000
60	2300.000	2100.000	1400.000	2100.000
80	3900.000	2800.000	2000.000	2800.000
100	6700.000	3800.000	2700.000	3800.000
120	11000.00	5200.000	3800.000	5200.000
140	20000.00	7000.000	5400.000	7000.000
160	33000.00	9500.000	7600.000	9500.000
180	57000.00	13000.00	11000.00	13000.00

Neck O.C.

As indicated above, the O.C. moment-angle characteristics were obtained from combining the neck column moment-angle characteristics with the characteristics of the O.C. cam/stop mechanism (Table 10).

Table 10. Occipital Condyle Joint Properties

Joint Angle (deg)	Extension Torque (in-lbs)	Adduction Torque (in-lbs)	Flexion Torque (in-lbs)	Abduction Torque (in-lbs)
0	0.000000	0.000000	0.000000	0.000000
20	80.00000	1120.000	150.0000	1120.000
40	480.0000	1500.000	700.0000	1500.000
60	980.0000	2100.000	980.0000	2100.000
80	1600.000	2800.000	1400.000	2800.000
100	2700.000	3800.000	1900.000	3800.000
120	4400.000	5200.000	2600.000	5200.000
140	7000.000	7000.000	3600.000	7000.000
160	11000.00	9500.000	5000.000	9500.000
180	16000.00	13000.00	6800.000	13000.00

Ankle

The ankle data were obtained from quasi-static dorsiflexion, plantarflexion, inversion, and eversion tests (Table 11). The function for torsion was also obtained from the Z-rotation data (Table 12).

Flexion Data:

Table 11. Ankle Joint Flexure Properties

Joint Angle (deg)	Extension Torque (in-lbs)	Adduction Torque (in-lbs)	Flexion Torque (in-lbs)	Abduction Torque (in-lbs)
0	0.000000	0.000000	0.000000	0.000000
20	0.000000	40.00000	220.0000	40.00000
40	0.000000	340.0000	839.9999	340.0000
60	350.0000	920.0000	1860.000	920.0000
80	830.0000	1760.000	3270.000	1760.000
100	1530.000	2880.000	5090.000	2880.000
120	2440.000	4260.000	7300.000	4260.000
140	3570.000	5920.000	9910.000	5920.000
160	4920.000	7840.000	12900.00	7840.000
180	6480.000	10000.00	16300.00	10000.00

Torsion Data:

The torsion moment-angle characteristic was considered the same in all azimuth directions, since the rotation is isolated from the other rotations.

Table 12. Ankle Joint Torsional Properties

Joint Angle (deg)	Torque (in-lbs)
0	0.000000
20	160.0000
40	2370.000
60	9100.000
80	19500.00
100	33600.00
120	51400.00
140	72900.00
160	98099.98
180	127000.0

The characteristics of the slip joints defined between the upper and lower femur segments (joined by the femur puck) and the upper and lower tibia (joined by the tibia puck) are given by spring force-deflection functions provided in the report on the force-deflection data.

2.4. THOR-NT Force-Deflection Data for Deformable Components

Unlike the previous generations of test manikins, THOR-NT has many deformable and flexible parts. Not all of them are modeled in ATB. However, some major ones are modeled using ATB's force-deflection functions. These functions are meant to be used with the type of contact surfaces found in the developmental experiments. They may require changes if the types of the contact surfaces are very different.

Force-deflection data were determined experimentally through indentation tests on the pelvis skin, femur skin, and tibia skin. Force-deflection characteristics of the femur puck and tibia puck were also determined. The pucks are represented by springs acting at the slip joint defined at these locations. The values obtained from the experiment were used provisionally. The final form of these functions were determined from the results of the knee impact test (for the femur puck) and the heel impact test (tibia puck), since the dynamic results were considered more important than the quasi-static results. Force-deflection characteristics for the head, face, upper thorax, lower thorax, and pelvis were determined from the corresponding certification test. The characteristics were estimated to allow for the best matching to the dynamic results. The force-deflection data for these segments are presented in the report on the simulations of the certification tests.

Pelvis Skin Force-Deflection

A six inch indentor was used to estimate the force-deflection characteristics, since the contact area is expected to be representative of the contact with the seat cushion and seat back. Compression tests were conducted on the bottom and the back of the pelvis skin (Table 13 and Table 14).

Pelvis Bottom

Table 13. Pelvis Bottom Skin Force-Deflection Data

Deflection (in)	Force (lbs)
0	0
0.5	38
0.75	64
1	110
1.25	240
1.5	760

Pelvis Back

Table 14. Pelvis Back Skin Force-Deflection Data

Deflection (in)	Force (lbs)
0	0
0.5	51
0.75	100
1	540
1.05	750

Femur Skin Force-Deflection

Compression tests on the femur skin were conducted with a three inch indentor. This again was considered representative of the contact area against the femur (e.g. with the seat cushion). Force-deflection characteristics for both the front and back of the femur were determined (Table 15 and Table 16).

Femur Front

Table 15. Femur Front Skin Force-Deflection Data

Deflection (in)	Force (lbs)
0	0
0.5	65
1	120
1.25	250
1.5	730
1.55	920

Femur Back

Table 16. Femur Back Skin Force-Deflection Data

Deflection (in)	Force (lbs)
0	0
0.5	15
1	39
1.5	87
1.75	150
2	400
2.1	610

Tibia Skin Force-Deflection

The compression tests on the tibia skin were conducted in the same manner as the femur skin. A three inch indentor was used for the tests. Data for both the front and back of the tibia were obtained (Table 17 and Table 18).

Tibia Front

Table 17. Tibia Front Skin Force-Deflection Data

Deflection (in)	Force (lbs)
0	0
0.25	2
0.3	6
0.35	49
0.4	140
0.45	450

Tibia Back

Table 18. Tibia Back Skin Force-Deflection Data

Deflection (in)	Force (lbs)
0	0
0.2	13
0.3	62
0.4	200
0.45	370
0.5	580

Femur Puck Force-Deflection

The joint at the femur separating the upper and lower segments is represented by a slip joint controlled by a spring. The force-deflection characteristics of the spring were determined quasi-statically. The force function is presented in the format required for the spring, i.e. with the compression characteristics as negative values for the deflection. The expansion of the neutral spring (i.e. tension) was not measured directly, but a nominal value of 50% of the initial compression slope was used (Table 19).

Table 19. Femur Puck Force-Deflection Data

Deflection (in)	Force (lbs)
-1	-8300
-0.8	-4800
-0.6	-2900
-0.4	-1800
-0.2	-1100
0	0
1	4150

Tibia Puck Force-Deflection

The joint at the tibia separating the upper and lower segments is represented by a slip joint controlled by a spring. The force-deflection characteristics of the spring were determined quasi-statically. The force function is presented in the format required for the spring, i.e. with the compression characteristics as negative values for the deflection. As in the case of the femur puck, the expansion of the neutral spring (i.e. tension) was not measured directly, but a nominal value of 50% of the initial compression slope was used (Table 20).

Table 20. Tibia Puck Force-Deflection Data

Deflection (in)	Force (lbs)
-1.2	2400
-1	-1500
-0.8	-950
-0.6	-580
-0.4	-370
-0.2	-230
0	0
1	2200

3. COMPARISON OF THOR-NT CERTIFICATION TEST AND ATB SIMULATION

There are a number of certification tests that are used to certify the proper response of the THOR-NT dummy. These tests involve impacts to different components of the dummy and verify the proper functioning of the deformable elements, such as the head skin, face foam, neck, thorax, abdomen, femur, and the lower legs (THOR-Lx). These certifications tests have been simulated using the ATB model for the THOR-NT.

The simulations serve a two-fold purpose. They are used to compare the predictions from the simulation model with the results of the actual test. In addition, the simulations are also used to tune the contact functions for the head, face, thorax, abdomen, femur, and leg. The description of each test and the assumptions made in the model are described below. The general guiding principle in the ATB models was to use the same functions whenever two tests involved the same segment. E.g. there are two tests involving the face, the disk impact, and rod impact. The same face function is used, so in this case an attempt is made to develop a function that has reasonable overlap with tests results from both these tests. The full-scale NT model is used for all tests except for the THOR-Lx certification (using only the lower leg assembly), and the neck certification (modeled using only a head/neck assembly). The functions are defined such that the minimum number of points was used. For most of the contacts, a damping function is also defined (using the rate-dependent feature of the contact definition in ATB). The damping functions were all constant, except for the one used for the sternal impact.

The certification tests are described in detail in the document: THOR-NT Certification Manual, Version 2005.1. This is available at the National Highway Traffic Safety Administration (NHTSA).

3.1. Head Impact Test

The head impact test consists of a 51.5 lb rigid impactor in the shape of a 6” disk impacting the top of the forehead of the whole dummy. The impact speed is 79 in/sec (2.0 m/s). The impactor was modeled as an ellipsoidal segment attached to a prescribed segment moving at the same speed. The attachment was through a free slip joint (Figures 2 & 3).

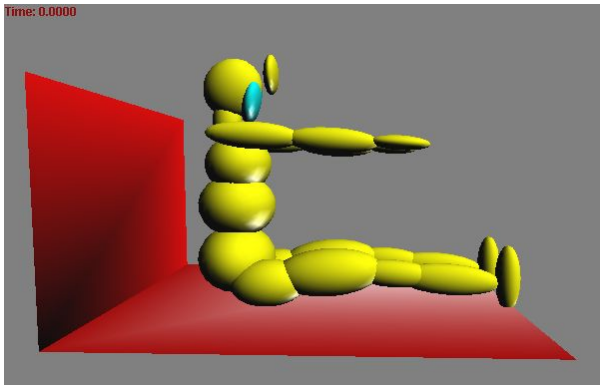

Figure 2. Initial Setup for Head Impact Simulation

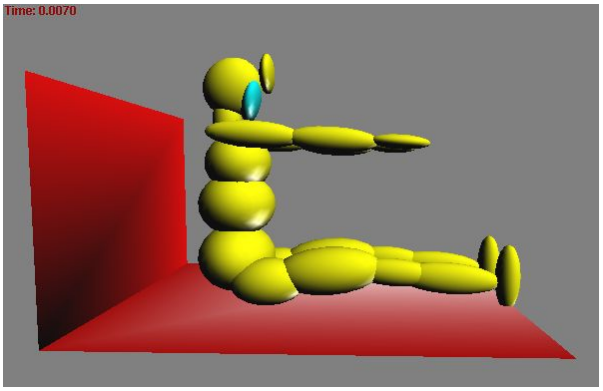

Figure 3. Head Impact at the Time of Peak Force

The simulation data compared reasonably well with the test data (Figure 4) after the head contact function was tuned.

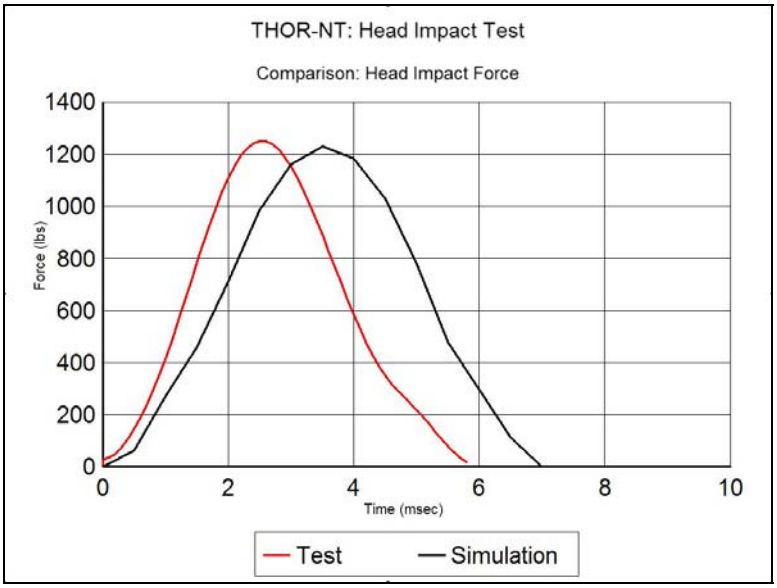

Figure 4: Comparison of Test and Simulation Force Data for Head Impact

The head contact function was tuned to provide the maximum peak force and approximate peak time. There was some difficulty in getting the correct rise time with only a contact function (Table 21) and friction function; a damping function was added to provide a closer match to the test.

Table 21. Head Contact Function

Deflection (in)	**Force (lb)**
0.0	0
0.1	500
0.2	1500
0.3	3500
0.35	5500

The damping coefficient (in the form of a function) was 0.5 lb/in/sec.

3.2. Face Disk Impact Test

The face disk impact test consists of a 29 lb rigid impactor in the shape of a 6” disk impacting the top of the center of the face of the whole dummy. The impact speed is 264 in/sec (6.7 m/s). The impactor was modeled as an ellipsoidal segment attached to a prescribed segment moving at the same speed. The attachment was through a free slip joint. The face has been modeled as an additional ellipsoid attached to the head in the THOR-NT model. The contact was set up with the additional ellipsoid, rather than the head (Figures 5 & 6).

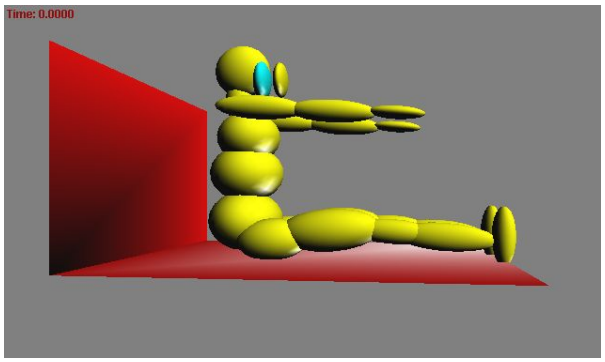

Figure 5: Initial Setup for Face Disk Impact

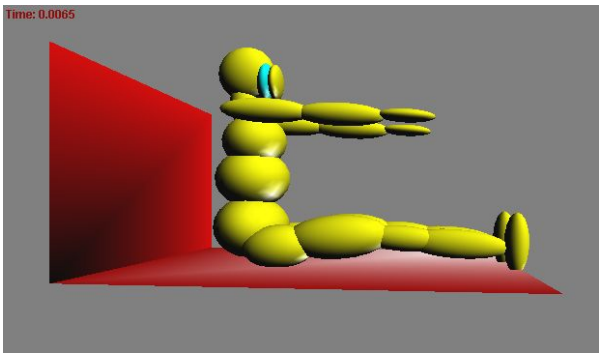

Figure 6: Face Disk Impact at Peak Force

The simulation results were compared with the test data (Figure 7).

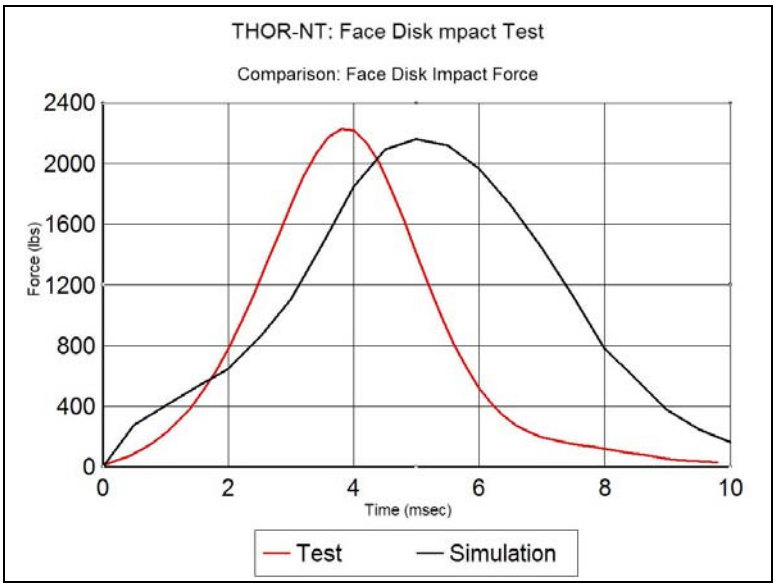

Figure 7: Comparison of Test and Simulation Data for Face Impact

The face contact function was tuned to provide the maximum peak force and approximate peak time. As in the case of the head function, a damping function was added to provide a closer match with test data. Also, the same function is used for the disk impact and the rod impact, the two certification tests involving the face. It was decided to use the face disk impact to tune the function since it was distributed over the whole face. The rod impact test would be modeled using the function developed here (Table 22).

Table 22. Face Impact Function; used for both disk and rod tests

Deflection (in)	**Force (lb)**
0.0	0
0.25	250
0.50	500
0.70	1000
0.90	2000
1.10	3000

The damping function used was a constant value of 2.0 lb/in/sec.

3.3. Face Rod Impact Test

The face rod impact test consists of a 70.4 lb rigid impactor in the shape of a 12" long cylindrical rod with a one inch diameter. The rod impacted the cheek area of the face, approximately at the center of the face of the whole dummy. The impact speed is 142 in/sec (3.6 m/s). The impactor was modeled as an ellipoisodal segment attached to a prescribed segment moving at the same speed (Figures 8 & 9). The attachment was through a free slip joint. The face has been modeled as an additional ellipsoid attached to the head in the THOR-NT model. The contact was set up with the additional ellipsoid, rather than the head.

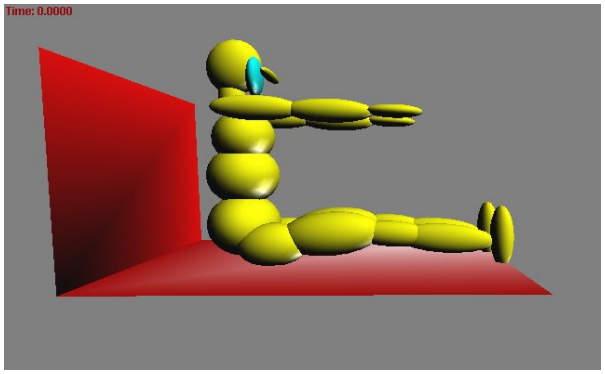

Figure 8: Initial Setup for Face Rod Impact

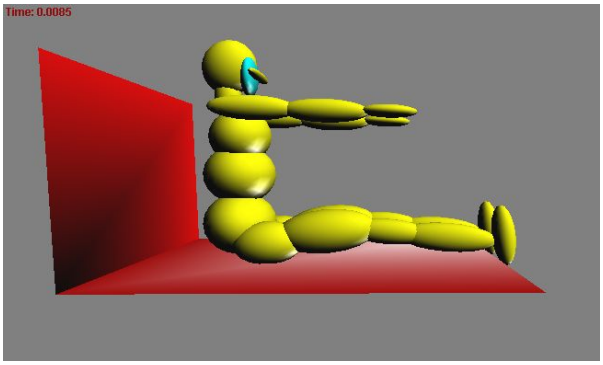

Figure 9: Face Rod Impact at Peak Force

As indicated in the discussion of the face disk impact, the same face contact function was used for both the disk and rod test. Since a standard contact has been defined, which depends on penetration and distance and not on area, it was not expected that we would get a fidelic simulation. But the peak is within the normal corridor and the timing and duration are reasonable (Figure 10). The main discrepancy is in the rise profile, with the simulation predicting a much more rapid rise (due to the damping function) than in the test. But this prediction is considered adequate for a lumped mass model.

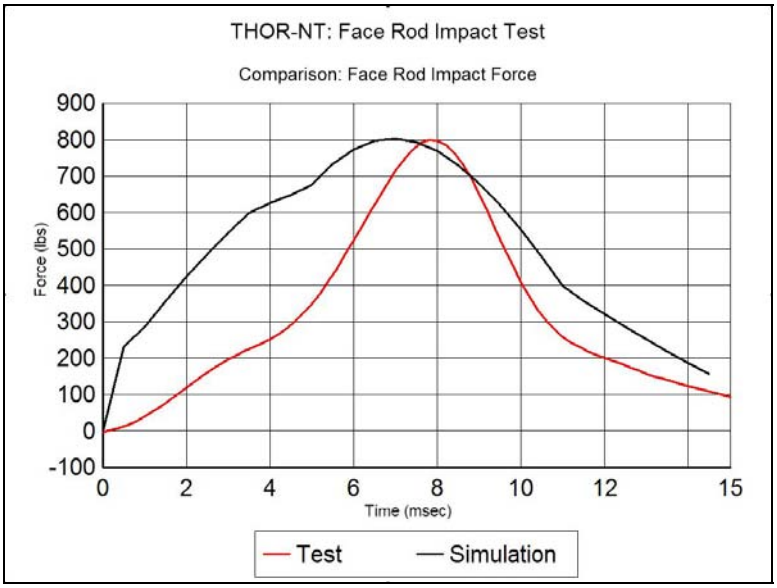

Figure 10: Comparison of Test and Simulation Force for Face Rod Impact

3.4. Sternal Impact Tests

There are two impact tests on the central sternum to verify the thorax response characteristics of the THOR-NT. These tests are alternatively known as the Kroell tests. A 51.5 lb impactor in the shape of a 6 inch disk is used to impact the sternum. Two impact speeds, at 169.4 in/sec (4.3 m/s) and at 264 in/sec (6.7 m/s) are used. The impactor was modeled as an ellipoisodal segment attached to a prescribed segment moving at the same speeds (Figures 11 & 12). The attachment was through a free slip joint.

The thorax impact response is characterized by fairly high damping, with a rapid force rise, a subsequent force plateau, and again a rapid force decrease (with large hysteresis). There are several lumped-mass models that provide a computer model of the dynamic behavior. The models (normally known as Lobdell models) consist of a number of spring damper systems, which connect a small sternal mass to a larger spine mass, as well as a contact function which describes the flesh/skin contact with the external impactor. For the current THOR-NT ATB model, a less complicated model was used. This consists only of a contact force-deflection function and a damping function. The aim of the functions was to provide a relatively accurate representation of the contact without adding too much modeling overhead, which could be used more reliably in other test configurations.

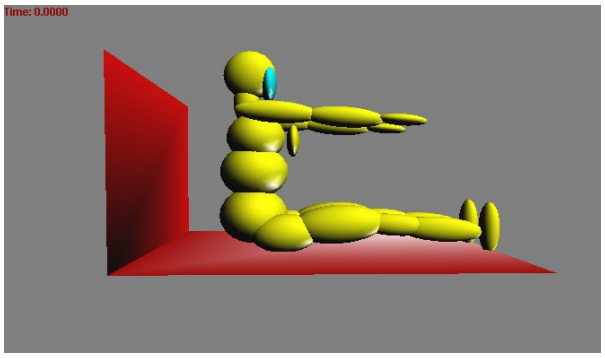

Figure 11: Initial Setup for Sternal Impact by Pendulum

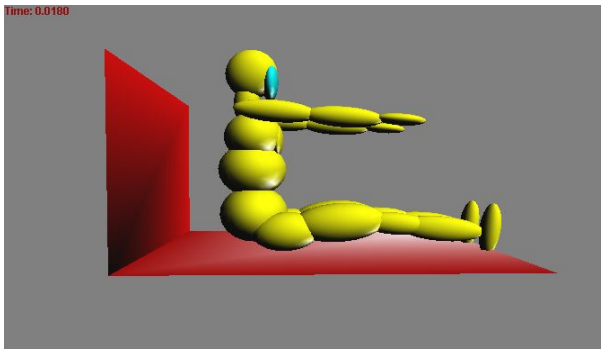

Figure 12: Sternal Impact at Peak Force

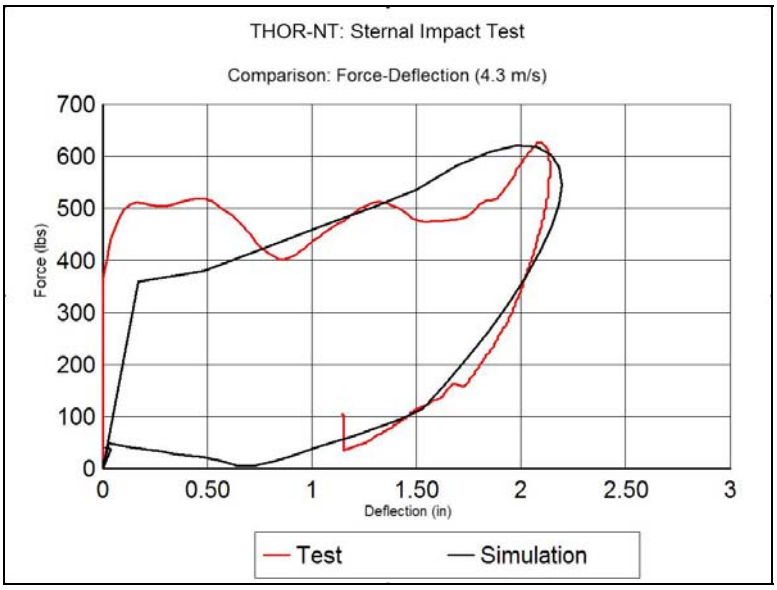

Figure 13. Comparison of Test and Simulation Force Data for Sternal Impact at 4.3m/s

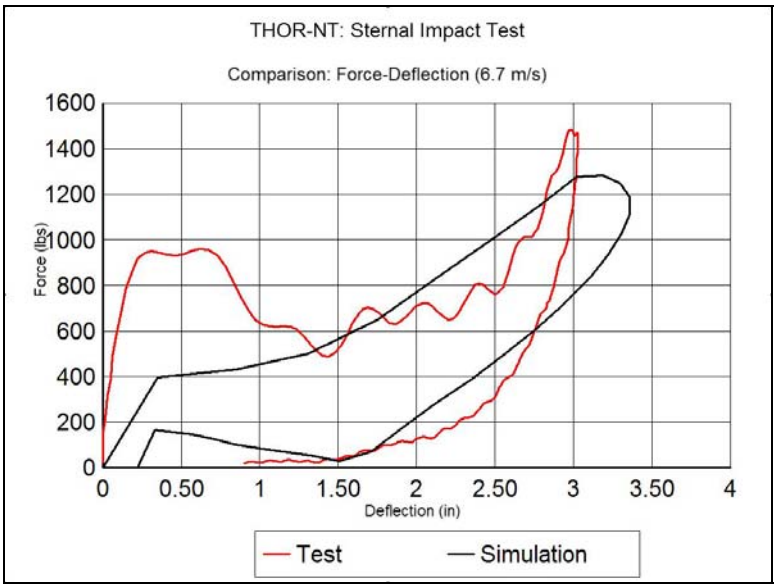

Figure 14. Comparison of Test and Simulation Force for Stern Impact at 6.7m/s

The thorax contact function and damping function were tuned to provide good representation at the 169.4 in/sec impact speed (Figure 13). The slower speed is considered more relevant in modern vehicle test configurations. It is seen that peak force, peak deflection, and hysteresis is well predicted at the lower speed (Figure 14). The same function provides reasonable representation of these parameters at the higher impact speed, though it is not as good a representation of the initial rise of force (Table 23).

Table 23. Thorax Contact Function

Deflection (in)	**Force (lb)**
0.0	0
1.5	225
2.5	675
3.5	1125

The damping function was defined to be slightly different during compression and expansion – 3.0 lb/in/sec during compression and 2.4 lb/in/sec during expansion. These values were slightly modified from the original Lobdell model (Table 24).

Table 24. Thorax Dampling Function

Deflection Rate (in/sec)	**Force (lb)**
-500	-1200
-100	-240
0	0
100	300

3.5. Lower Ribcage (Thorax) Oblique Impact Test

The oblique impact test to the lower ribcage or thorax (also known as the MCW test in the THOR-NT Certification Manual) consists of a 51.5 lb impactor in the form of a 6 inch disk impacting the lower thorax of the full dummy at an angle of about 15 degrees to the spine. The impact speed is 169.4 in/sec (4.3 m/s). The impactor was modeled as an ellipoisodal segment attached to a prescribed segment moving at the same speeds. The attachment was through a free slip joint. The 15 degree rotation was achieved by rotating all the segments of the whole dummy about the Z axis by this amount (Figures 15 & 16).

.

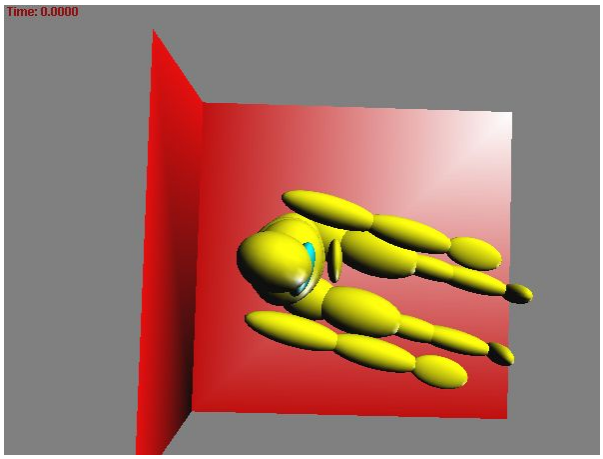

Figure 15: Initial Setup for Lower Ribcage Oblique Impact

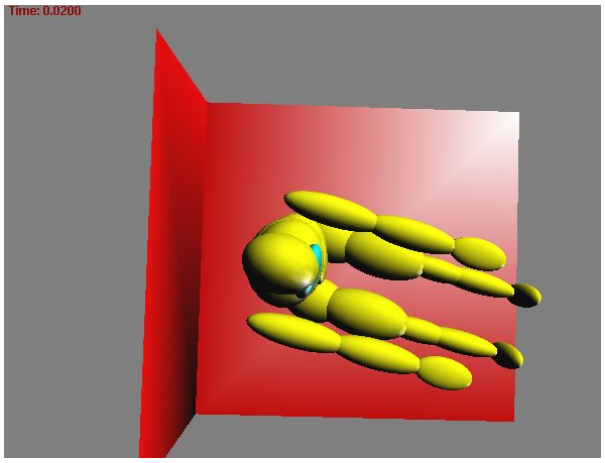

Figure 16: Lower Ribcage Oblique Impact at Peak Force

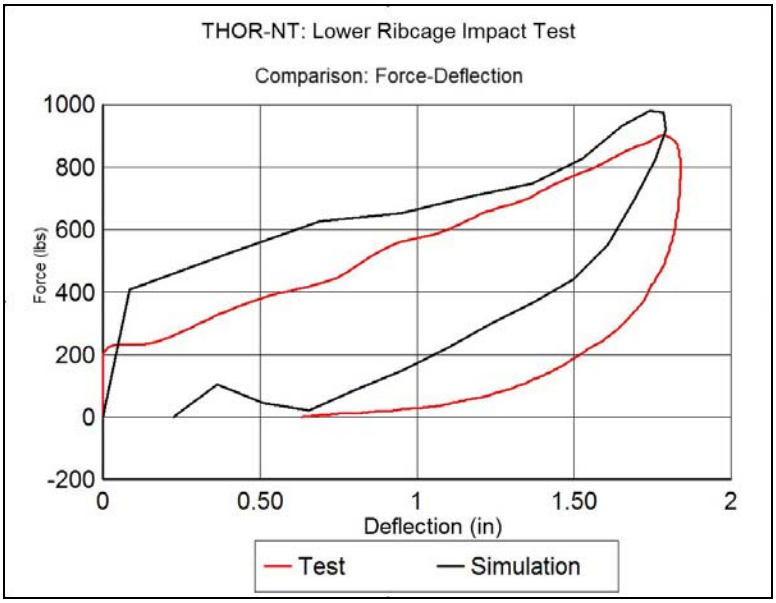

Figure 17. Comparison of Test and Simulation Force-Deflection Data for Lower Ribcage Oblique Impact

The lower thorax contact force and damping functions were tuned to provide a match of the peak force and deflection. It is seen that both the peak force and deflection, as well as hysteresis, is fairly well predicted (Figure 17). The same contact function is used for both the lower ribcage impact and the upper abdomen impact, which both involve contact with the lower ribcage or thorax (Table 25). The aim of the contact model for the lower thorax was to simulate both conditions as well as possible.

Table 25. Upper Abdomen (Lower Thorax) Contact Function

Deflection (in)	**Force (lb)**
0.0	0
1.50	600
2.00	1200
2.75	4800

The damping function was constant with a value of 2.0 lb/in/sec.

3.6. Upper Abdomen Impact Test

The upper abdomen impact test uses a steering wheel shaped impactor which impacts the middle of the upper abdomen. The impactor mass is 40 lbs and the impactor speed is 315 in/sec (8.0 m/s). The steering wheel diameter is 13 inches and is oriented at an angle of 30 degrees with respect to the vertical (Figures 18 & 19). The impactor was modeled as an ellipoisodal segment attached to a prescribed segment moving at the same speeds. The attachment was through a free slip joint.

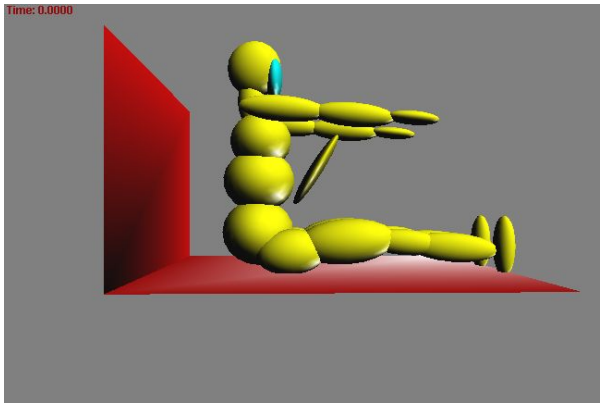

Figure 18: Initial Setup for Upper Abdomen Impact

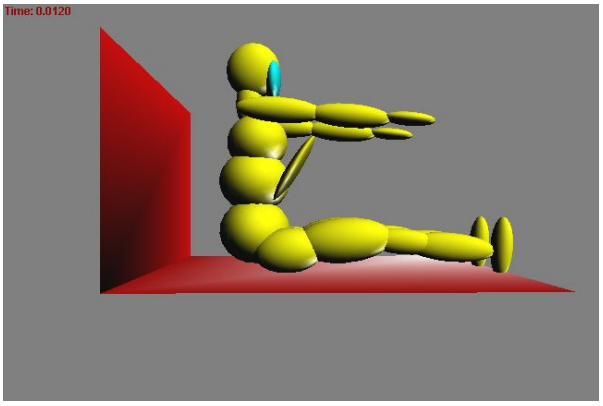

Figure 19. Upper Abdomen Impact at Peak Force

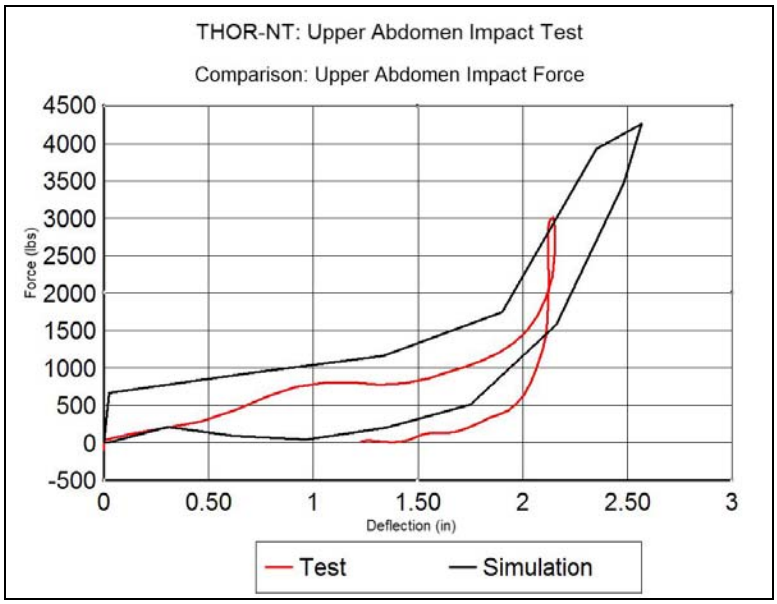

Figure 20: Comparison of Test and Simulation Force-Deflection for Upper Abdomen Impact Test

As indicated in the description of the lower ribcage test, the same contact function developed for that test is also used in this case. Since the impactor shape is narrow and angled, it was expected there would be some discrepancy between the simulation and test responses for this test (Figure 20). It is seen that the general shape of the response is reproduced, but the initial rise due to the damping function and the final peak force are too high. Since this is a very high velocity impact (315 in/sec), the higher damping force and peak force are expected.

3.7. Lower Abdomen Impact Test

The lower abdomen impact is carried out using a 12 inch cylindrical rod, with a one inch radius. The impactor mass is 70.4 lbs and the impactor speed is 240 in/sec (6.1 m/s). The impactor was modeled as

an ellipoisodal segment attached to a prescribed segment moving at the same speeds. The attachment was through a free slip joint. Because the one inch diameter for such a long ellipsoid was considered to make the contact algorithm somewhat unstable, the diameter was increased to 1.5 inch (Figures 21 & 22). Since the contact algorithm does not depend on the contact area but only on penetration, this change was not considered to make any significant change to the predicted response.

The display at peak force is not shown, in this case, because the impactor is hidden by the pelvis segment (only the outer edge is visible in the figure on the bottom).

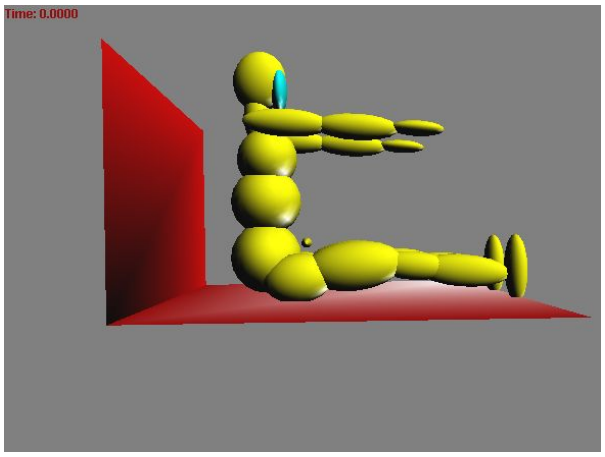

Figure 21: Initial Setup for Lower Abdomen Rod Impact

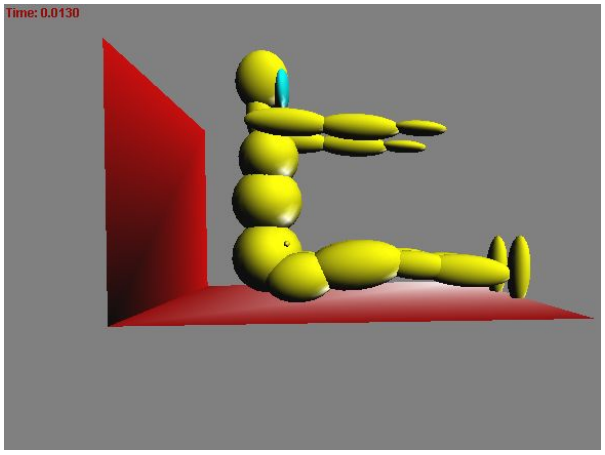

Figure 22: Simulation Display of Lower Abdomen Rod Impact at Peak Force

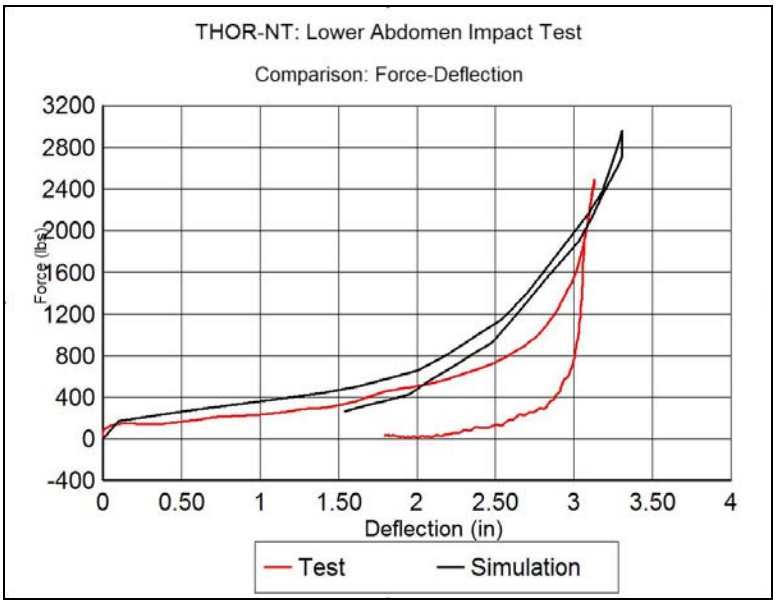

Figure 23: Comparison of Test and Simulation Force-Deflection for Lower Abdomen Impact

There was some difficulty in defining the force-deflection for the lower abdomen contact. The force shows a slow rise but a fair amount of hysteresis. The use of R and G factors was not considered suitable in this case because the hysteresis was not smooth (Figure 23). Only a small amount of damping was used in the damping function, since increasing the damping would also increase the initial force. The choice was a compromise to get the approximate shape and peak (Table 26).

Table 26. Lower Abdomen (Pelvis) Contact Function

Deflection (in)	**Force (lb)**
0.0	0
1.5	300
2.0	500
2.5	1000
3.0	2000
3.25	3000
3.50	5000

The damping was defined to be 0.6 lb/in/sec.

3.7. Femur Impact Test

The femur impact test consists of an impact to the knee along the axis of the femur. The impactor mass is 11 lbs and the impactor shape is in the form of a disk with a diameter of 3 inches. The impactor speed is 102 in/sec (2.6 m/s). The impactor was modeled as an ellipoisodal segment attached to a prescribed segment moving at the same speeds (Figures 24 & 25). The attachment was through a free slip joint. The impact is applied to the whole dummy and the force through the femur is modulated by the spring attached between the upper and lower femurs connected through the femur slip joint. Thus the impact

involves both the contact function at the knee and the force-deflection characteristics of the spring at the femur slip joint.

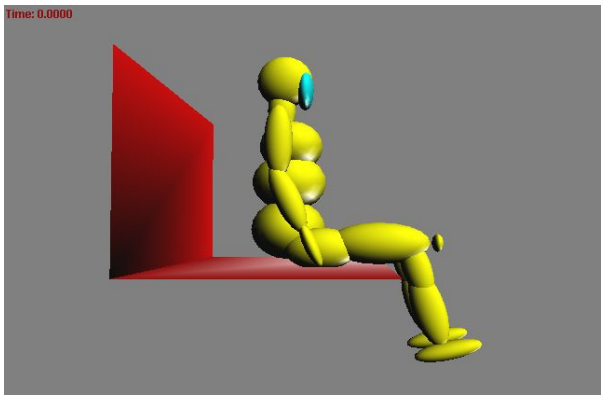

Figure 24: Initial Setup for Femur/Knee Impact

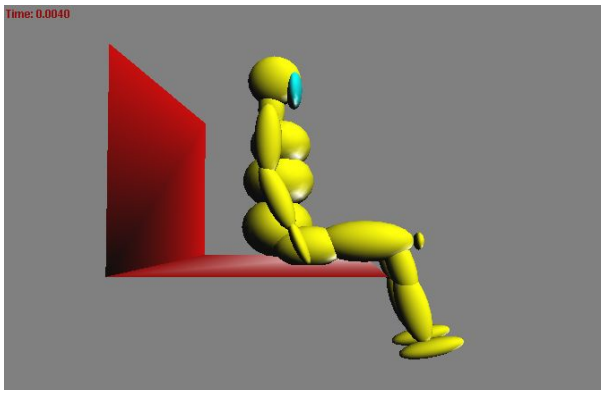

Figure 25: Femur/Knee Impact at Peak Force

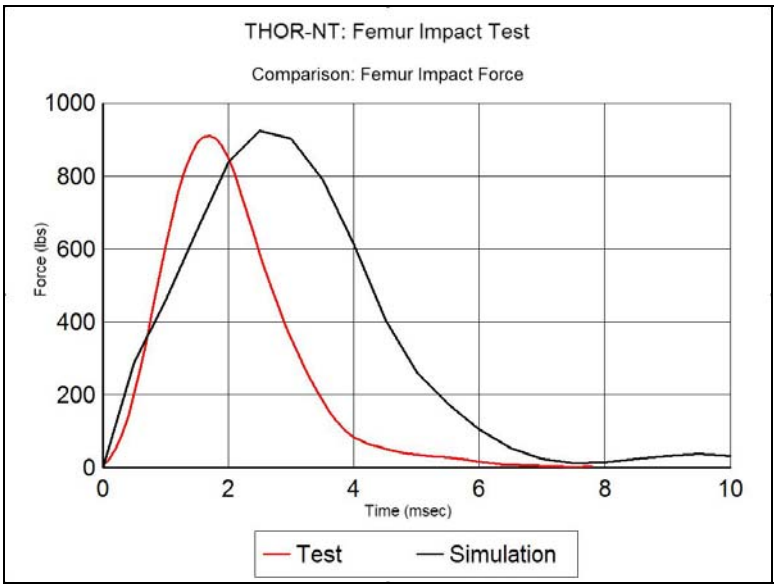

Figure 26: Comparison of Test and Simulation Force Data for Femur/Knee Impact

The peak force and approximate peak time were predicted fairly well, but the unloading is seen to be delayed in the simulation (Figure 26). As mentioned above, the complete response is a combination of the force-deflection characteristics at the knee and the spring characteristics of the femur puck connecting the upper and lower femur segments. The femur puck characteristics were kept unchanged from the data obtained from the compression tests on the puck. The knee characteristics were tuned to provide a good peak force (Table 27). It was difficult to control the damping function to match both the loading and unloading characteristics.

Table 27. Knee Contact Function

Deflection (in)	Force (lb)
0.0	0
0.1	400
0.2	1200
0.25	2000
0.27	3000

The damping was defined to be 1.5 lb/in/sec.

3.8. THOR-Lx Impact Tests

There are two impact tests that are used to certify the THOR-NT lower leg, also known as THOR-Lx. There are also two quasi-static tests to certify the inversion/eversion characteristics, but these are difficult to model through the ATB simulation.

3.8.1. Heel Impact Test

The first is an impact to the plantar surface of the foot, known as the heel impact, which acts through the axis of the tibia. It uses a pendulum driven impactor in the shape of a rigid hemi-cylinder. The effective impactor mass is 11 lbs and the impactor speed is 169.4 in/sec (4.0 m/s). The test is performed only on the THOR-Lx assembly, with the upper tibia (at the upper tibia load cell) rigidly attached to a support plate. The simulation model consists of the segments upper tibia, lower tibia, and foot (Figures 27 & 28). The impactor was modeled as an ellipoisodal segment attached to a prescribed segment moving at the same speeds. The attachment was through a free slip joint. The THOR-Lx tibia consists of the upper and lower tibia segments joined by a rubber tibia puck. The puck is modeled as the tibia joint, and is defined by a slip joint, and represented by a spring. The force generated by the heel impact involves the combination of the heel contact function and the spring function at the tibia joint.

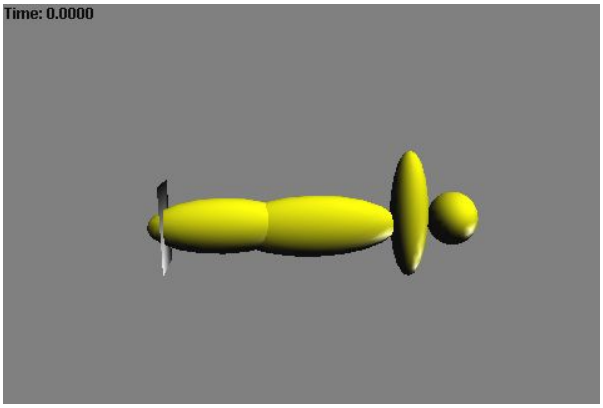

Figure 27. Initial Setup for Heel Impact

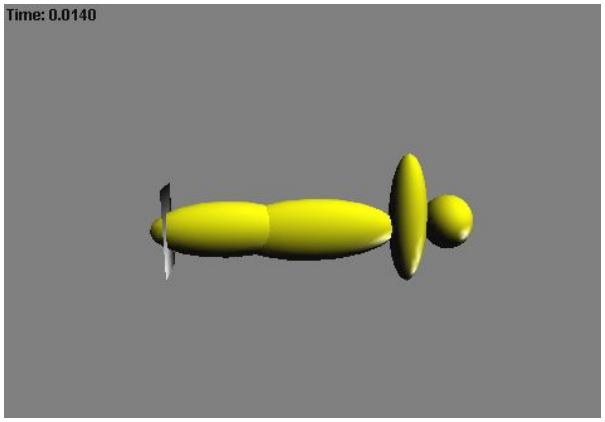

Figure 28. Heel Impact at Peak Force

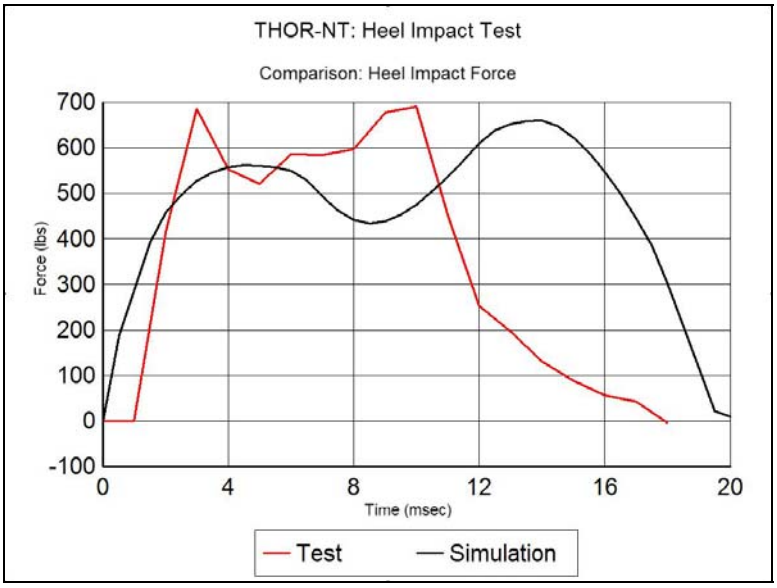

Figure 29: Comparison of Test and Simulation Force Data for Heel Impact

The simulation produces the same peak force, the time of initial peak, and approximately the rough shape of the response (Figure 29). It shows a double peak, arising from the compression of the heel through the heel contact function (Table 28) followed by the compression of the tibia joint spring. The simulation also produces the approximate duration of the curve, but does not correctly predict the difference in times between the two curves. Once again, the simulation predicts a much slower unloading, which is a common feature of lumped mass models and finite element models.

Table 28. Foot Contact Function

Deflection (in)	**Force (lb)**
0.0	0
0.2	500
0.4	820
0.6	1380
0.8	2200
1.0	3800
1.2	6600

Damping of 1.0 lb/in/sec was used for the contact. The force-deflection characteristics of the tibia puck were kept unchanged from those obtained from the compression tests.

3.8.2. Dynamic Dorsiflexion Test

The second impact test to certify the THOR-Lx is an impact to the ball of the foot so that the foot is driven into dorsiflexion. The test uses the same pendulum fixture with the same impactor mass. The impact speed is 197 in/sec (5.0 m/s). As for the heel impact, the test is performed on the THOR-Lx assembly, with the tibia (below the tibia puck) rigidly attached to a support plate. The simulation model consists of the segments upper tibia, lower tibia, and foot (Figures 30 & 31). In this case, the tibia puck, which is modeled as a slip joint with a spring, is locked so the same data set can be used. The axial force and moment generated by the dorsiflexion impact involve the joint properties of the ankle. The ankle properties are modeled using the ankle joint function (Table 29).

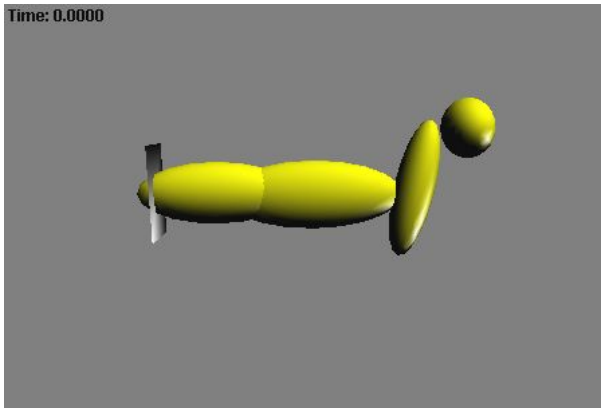

Figure 30: Initial Setup for Dynamic Dorsiflexion Test

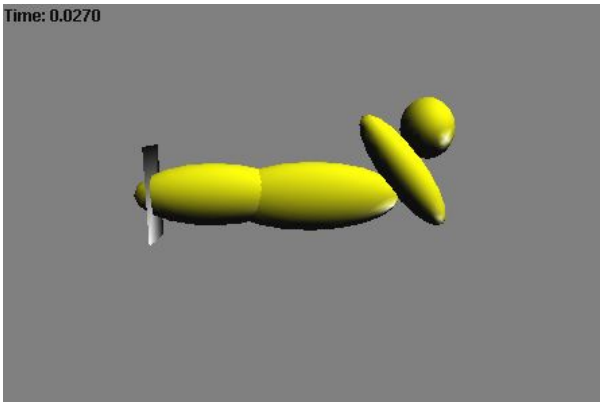

Figure 31: Dorsiflexion Test at Peak Force

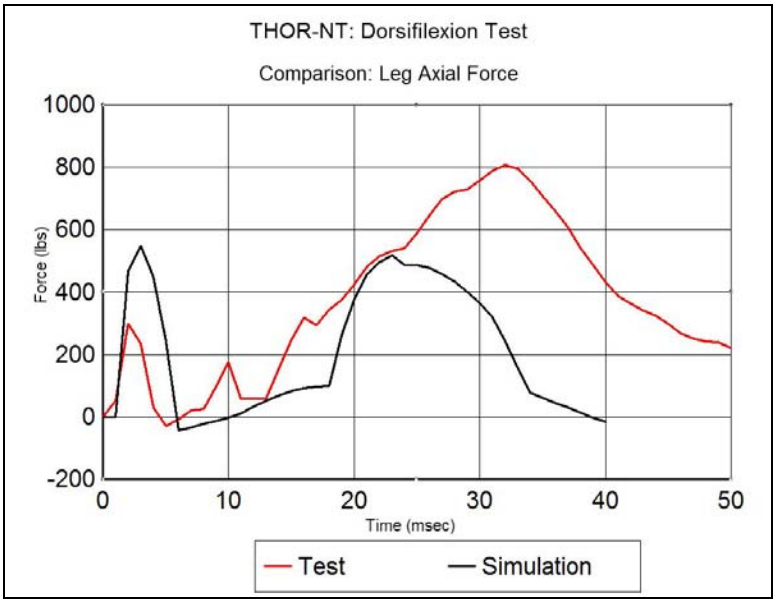

Figure 32: Comparison of Test and Simulation Tibia Axial Force for Dynamic Dorsiflexion Test

The same heel contact function used in the heel impact test was also used in this test. It is seen that the approximate shape is reproduced, i.e. an initial peak, followed by a second peak. But the peak force is not well predicted, or the peak time (Figure 32).

The second output from the test is the moment at the ankle vs. the angle of the foot with respect to tibia (Figure 33).

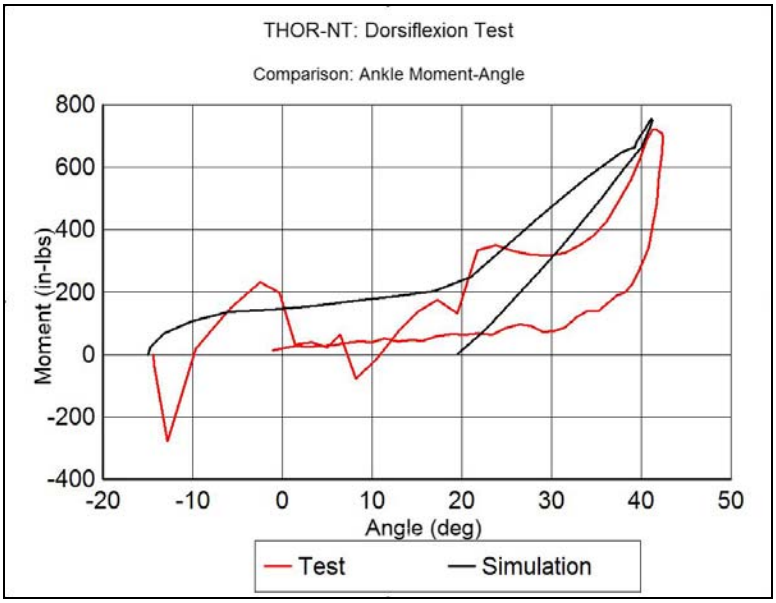

Figure 33: Comparision of Test and Simulation Moment of Ankle Response Data for Dynamic Dorsiflexion Test

The viscous coefficient for the ankle joint was tuned to provide a representation of the hysteresis seen in the test. It was also found that the original ankle joint function obtained from the quasi-static test had to be modified. The value of the moment at the lower angles was reduced (0 – 40 degrees), to get the best agreement. It is seen that the general shape is reproduced, along with the peak moment and peak angle. The oscillations seen in the test are not reproduced.

The ankle joint function was modified only in dorsiflexion.

Table 29. Ankle Joint Function Used for Dynamic Dorsiflexion Test

Angle (deg)	**Moment (in-lb)**
0	0
20	100
40	700
60	1860
80	3270
100	5090
120	7300
140	9910
160	12900
180	16300

The moments at 20 deg and 40 deg were originally set at 220 in-lb and 840 in-lb. The moments at the higher angles remained unchanged. The viscous coefficient for the ankle joint was set at 0.03 in-lb/deg/sec.

3.9. Neck Certification Tests

There are three neck certification tests that were conducted with a head/neck assembly attached to a standard head/neck pendulum (also used for Hybrid III neck testing). The pendulum was modeled as a rigid body joined to the laboratory system (base vehicle) through a pin joint. The length of the pendulum and its mass correspond to the standard pendulum length and mass (70 inch, 75 lbs). The loading on the base of the neck is determined by the pendulum acceleration, which is measured at a point 60 inches from the rotation point.

The three tests that are conducted to evaluate the response of the THOR-NT neck are the frontal flexion, extension and lateral flexion tests. Each test has a slightly different acceleration profile acting on the neck base. The acceleration is generated in the model (as in the test) through a contact function representing the force-deflection characteristics of the foam used to decelerate the pendulum. The force-deflection function was basically tuned using the frontal flexion test and the same function used for the other two test configurations. An alternative method for modeling the tests would have been to assign a prescribed acceleration for the base of the neck which would have been taken from the known acceleration profile. But it was considered that a more basic model which would generate the acceleration profile through a contact function would be more helpful.

Though the original tests involved releasing the pendulum from different heights, it was considered inefficient to employ this method to perform the simulations, since it would involve long simulation times. Instead, an initial angular velocity was assigned to the moving segments (pendulum and all attached head/neck segments) such that the consequent contact of the pendulum with the foam would generate the required acceleration. The different levels of the acceleration pulse for the three tests, were controlled using different initial angular velocities (while the contact function remained the same).

The THOR-NT neck assembly consists of front and rear neck springs in addition to the neck column. These provide a mechanical model of the front and rear muscles. The springs are compressed through cables which pass through the springs and outside the neck column and tied at the bottom of the base of

the neck. The initial model of the neck, to be used for the neck pendulum testing, was developed in DYNAMAN. An earlier model had been developed during the design phase, and the neck characteristics were updated with the properties measured for the THOR-NT neck. In order to model the neck springs and cables, two spring/dampers are modeled connecting two small mass segments (with the inertial properties of the springs) to the base of the head. The cables are modeled using two harness belts which connect the two new mass segments and are passed through slip rings which model the holes in the neck plates through which the real cables pass.

A difficulty was encountered when the model with the spring/dampers was modified to run with the ATBV3 program (the DYNAMAN program has a special feature to model slip rings). The procedure described in the ATBV3 Input Description document (ATBv3_inp_dscr.pdf: page 79-80) was used, where a negative value for the NF(5) function should model a slip ring. The input data file produced did not run properly, and a simpler model without spring/dampers was developed to run with the ATBV3 program. Because the spring/dampers were absent, the joint function at the O.C. was modified to include the effects of the front and rear spring dampers. Only the moment-angle properties for frontal flexion and extension were modified, while the lateral properties are unchanged. The results from both types of simulations (i.e. without and with spring/dampers) are presented below for comparison

3.9.1. Frontal Flexion Test

The peak deceleration in the frontal flexion test was ~ 25 g with a peak time of ~ 20 msec and duration of 40 msec. An initial angular velocity of 115 deg/sec was set for the pendulum and all other attached segments (Figures 34 & 35).

The following show the setup of the frontal flexion simulation at the start time and at point of maximum head rotation.

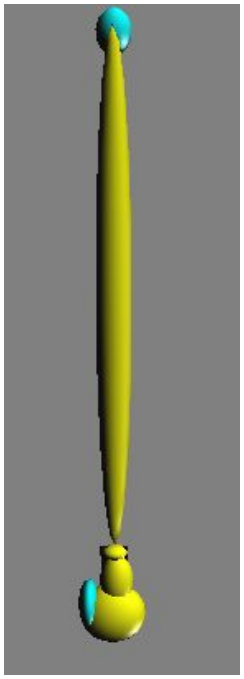

Figure 34: Initial Setup of Neck Flexion Test

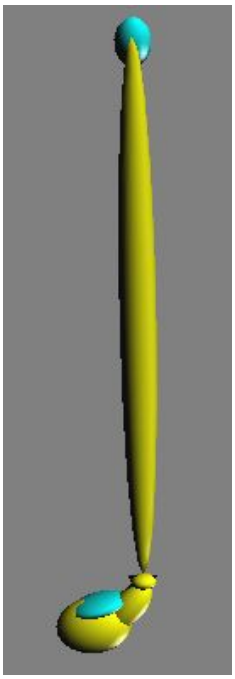

Figure 35: Neck Flexion Test at Peak Angle

The following graphs show the comparison of the pendulum acceleration, moment at O.C. (in Y direction), and the force in the X direction obtained for the model without spring dampers and run using the ATBV3 Program (Figures 36, 37, & 38).

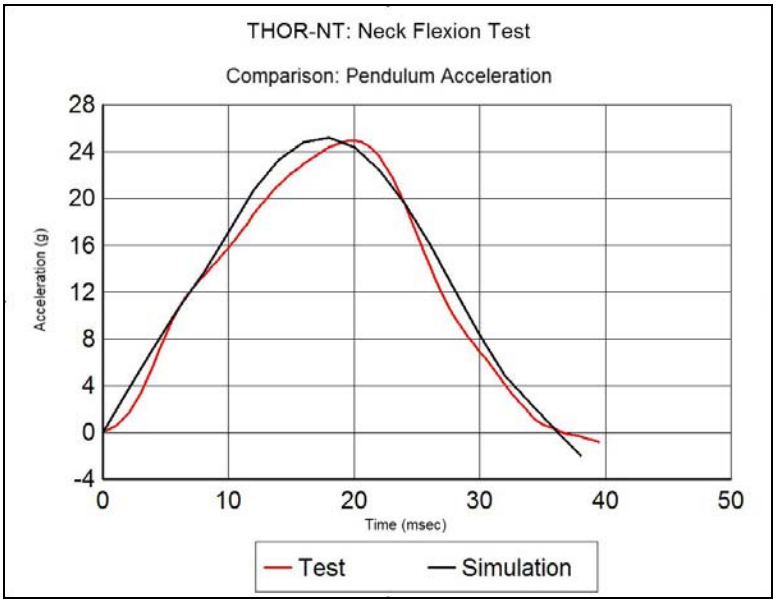

Figure 36. Comparison of Test and Simulation Pendulum Acceleration Data for Neck Flexion Test (without Spring/Cable Model)

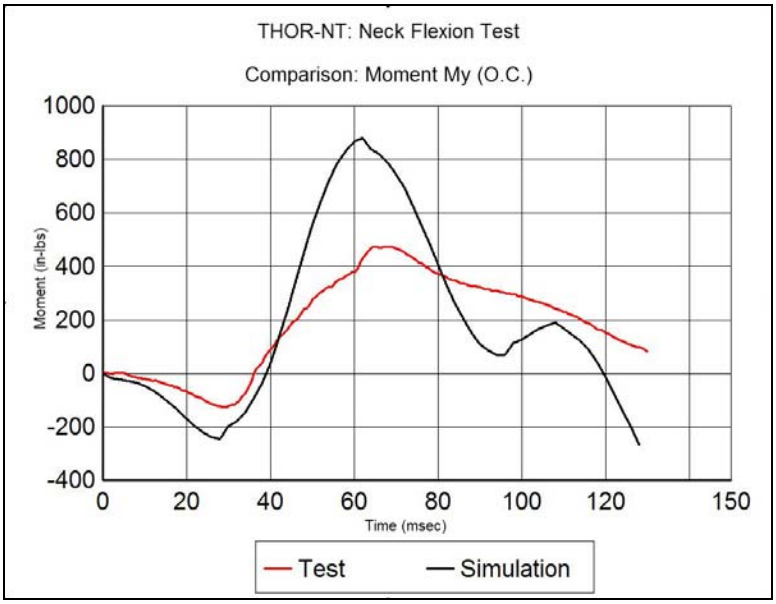

Figure 37. Comparison of Test and Simulation O.C. Moment Data for Neck Flexion Test (without Spring/Cable Model)

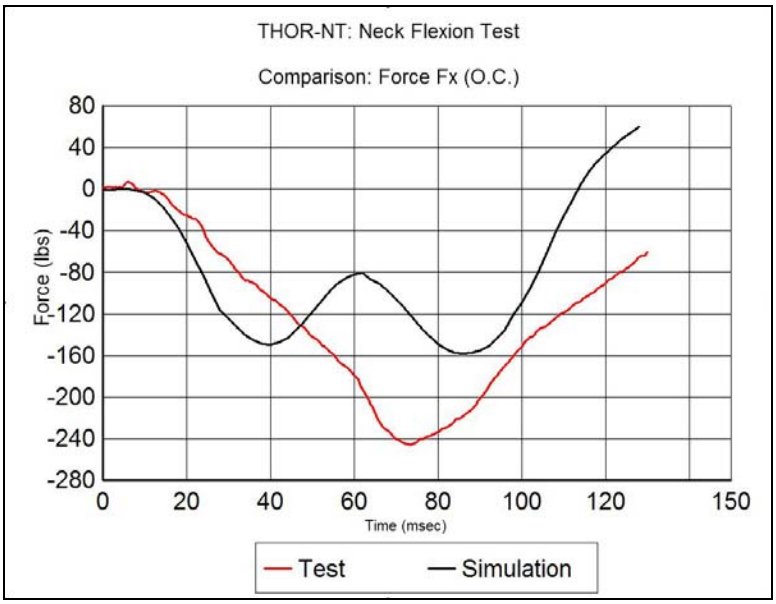

Figure 38. Comparison of Test and Simulation Fx Force at O.C. for Neck Flexion Test (without Spring/Cable Model)

The figures above show that the acceleration profile is reproduced well, and though the shapes of the My and Fx graphs from the simulation are generally similar to those from the test, the peaks are different and the Fx curves show two peaks which are absent in the test data.

The following show the results from the model with the spring/dampers using DYNAMAN. The neck spring data are also displayed (Figures 39, 40, & 41).

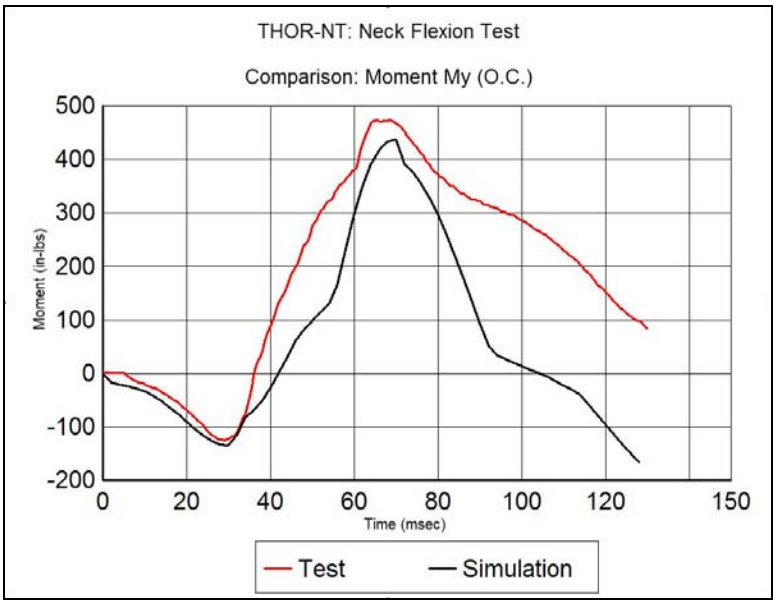

Figure 39. Comparison of Test and Simulation My at O.C. for Neck Flexion Test (with Spring/Cable Model)

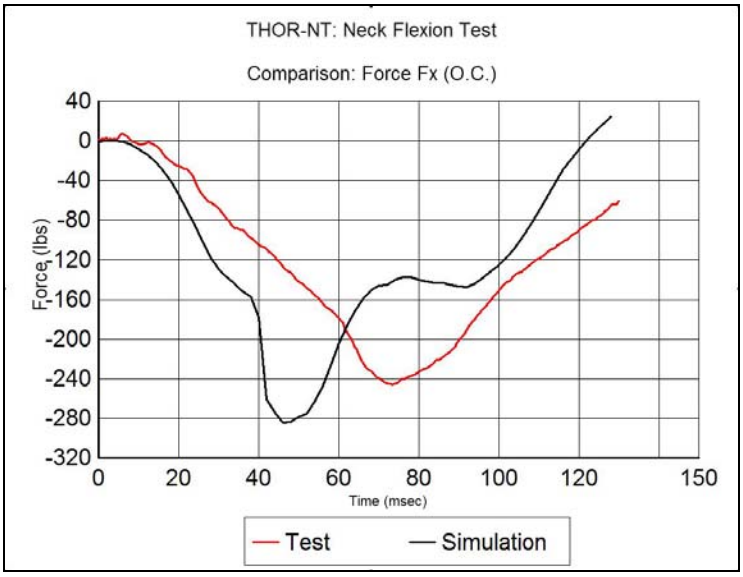

Figure 40. Comparison of Test and Simulation Fx at O.C. for Neck Flexion Test (with Spring/Cable Model)

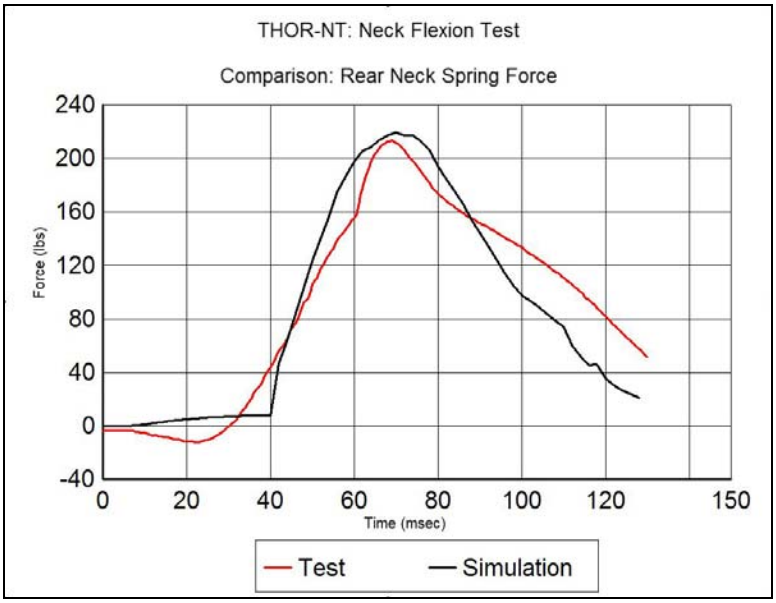

Figure 41. Comparison of Test and Simulation Rear Neck Spring Force for Neck Flexion Test (with Spring/Cable Model)

The figures above show that the acceleration profile is reproduced well, and though the shapes of the My and Fx graphs from the simulation are generally similar to those from the test, the peaks are different and the Fx curves show two peaks which are absent in the test data.

The simulation results with the spring/damper show a better match with the test data, though there is discrepancy in peak timing for the Fx graph (Figure 41). The spring model appears to match well with the spring test data.

3.9.2. Extension Test

The peak deceleration in the extension test was ~ 25 g with peak time of ~ 20 msec and duration of 40 msec. An initial angular velocity of 110 deg/sec for the pendulum and all other attached segments was prescribed (Figures 42 & 43).

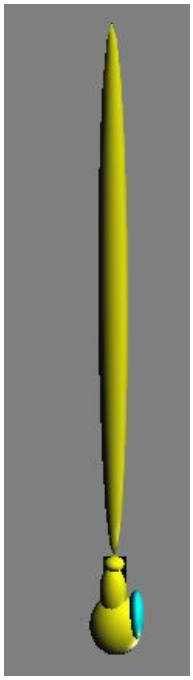

Figure 42. Initial Setup of Neck Extension Test

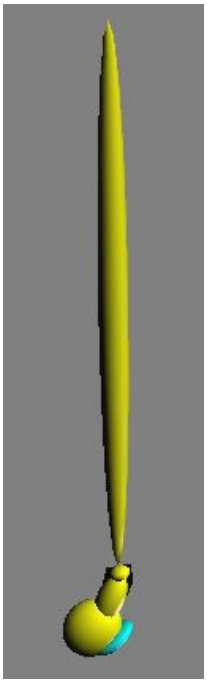

Figure 43. Neck Extesion Test at Peak Angle

The following graphs show the comparison of the pendulum acceleration, moment at O.C. (in Y direction), and the force in the X direction obtained for the model without spring dampers and run using the ATBV3 program (Figures 44, 45, & 46).

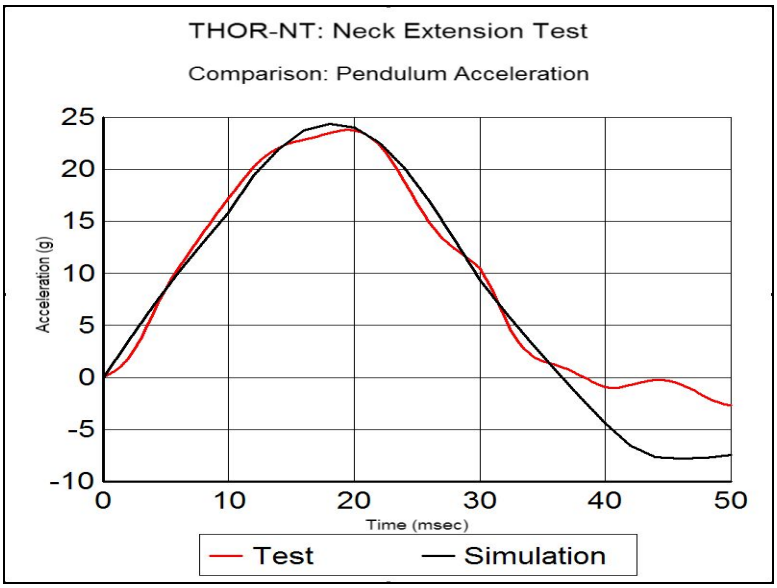

Figure 44. Comparison of Test and Simulation Neck Pendulum Acceleration for Neck Extension Test

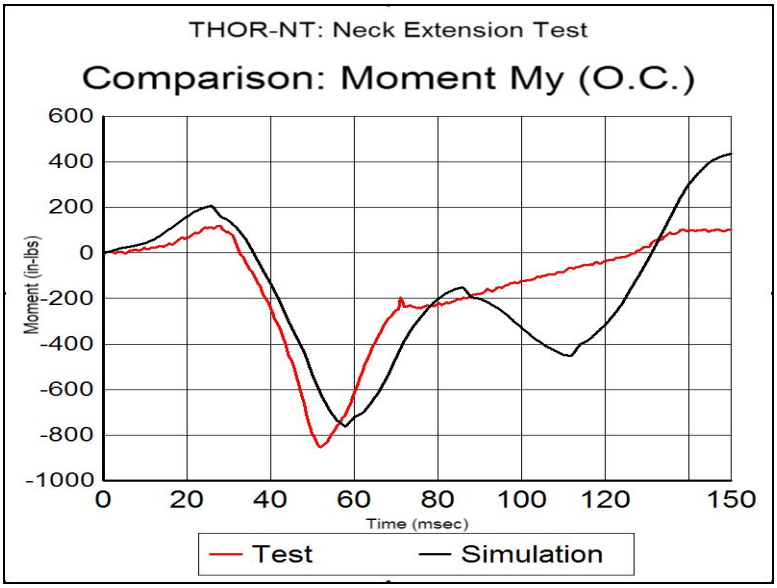

Figure 45. Comparison of Test and Simulation My at O.C. for Neck Extension Test (without Spring/Cable Model)

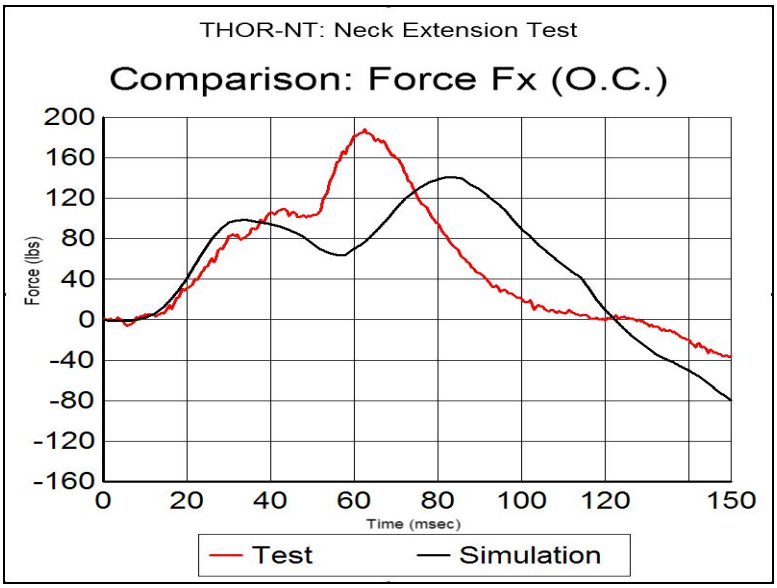

Figure 46. Comparison of Test and Simulation Fx at O.C. for Neck Extension Test (without Spring/Cable Model)

The figures above show that the acceleration profile for extension is reproduced well (Figure 44). There is good match of the main peak of the My response (Figure 45), though the simulation shows a smaller secondary peak. There is only general agreement for the Fx response (Figure 46). The simulation shows two distinct peaks, while the test shows only a slight first peak and a well defined second peak. The peak magnitude is within 30% of the test value.

The following show the results from the model with the spring/dampers using DYNAMAN. The neck spring data are also displayed (Figures 47, 48, & 49).

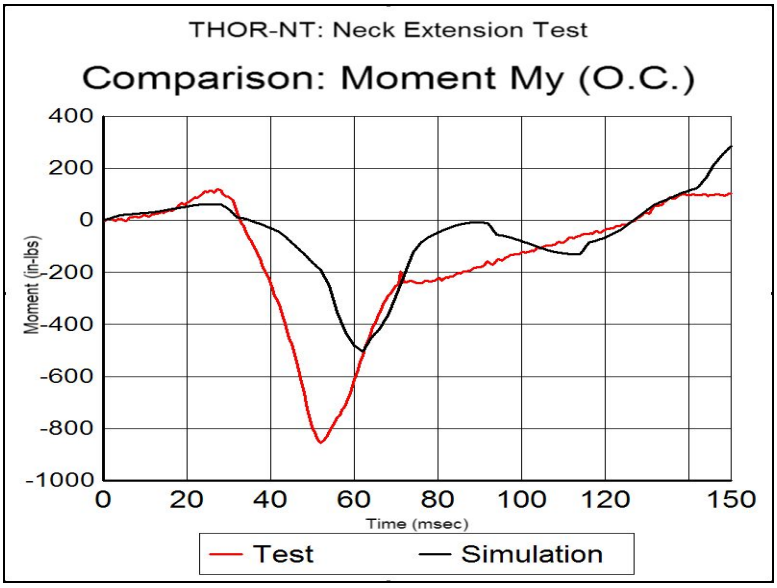

Figure 47. Comparison of Test and Simulation for My at O.C. for Neck Extension Test (with Spring/Cable)

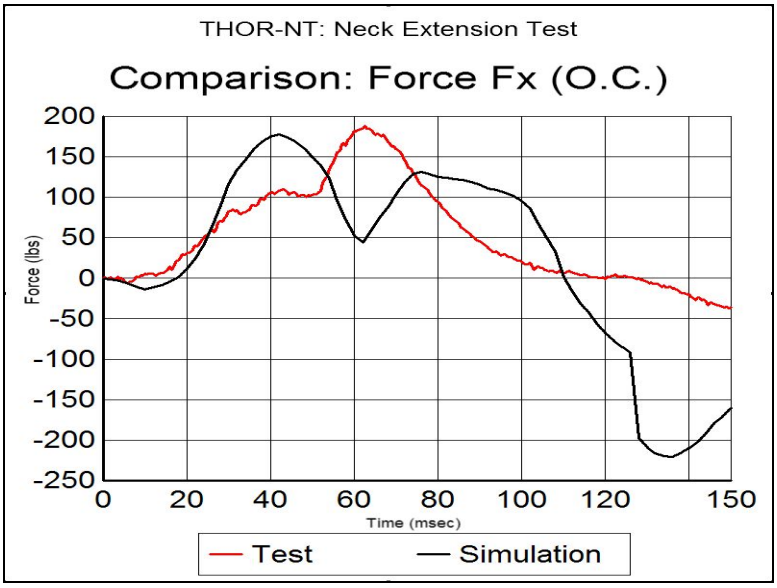

Figure 48. Comparison of Test and Simulation for Fx at O.C. for Neck Extension Test (with Spring/Cable)

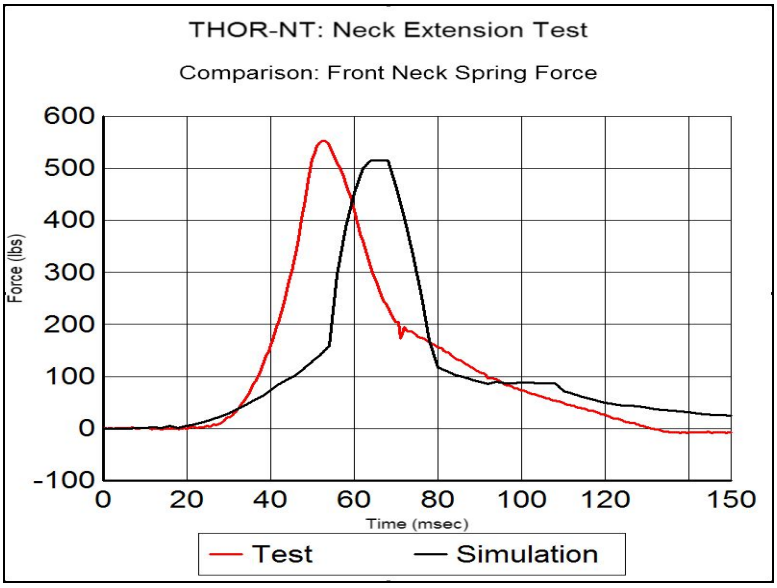

Figure 49. Comparison of Test and Simulation Front Neck Force for Neck Extension Test (with Spring/Cable Model)

The results with the spring/damper model show that the My response is not well represented (Figure 47), though the general shape is generated (and the secondary peak is relatively smaller than the model without the spring/damper). The Fx response is better modeled (Figure 48), with the peak well matched but occurring earlier than in the test. The front spring force is modeled fairly well, though being delayed relative to the test (Figure 49).

It is interesting to note, that the model without the spring/damper does a better job in modeling My. This may be related to the relatively stiff mechanism at the bottom of the neck column arising from the two small stops at pucks # 4 and #5. These are not modeled, and incorporated in the general neck joint functions and distributed evenly to the top and bottom of the neck.

3.9.3. Lateral Flexion Test

The peak deceleration in the lateral flexion test is in the range 15-17 g with peak time of ~ 22 msec and duration of ~44 msec. There is an initial angular velocity of 85 deg/sec for the pendulum and all other attached segments (Figure 50 & 51).

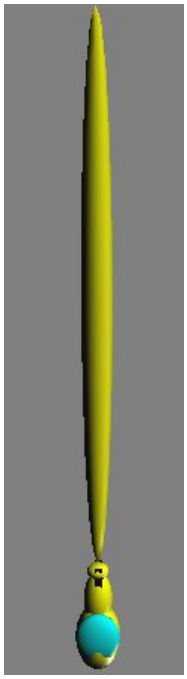

Figure 50. Initial Setup of Neck Lateral Flexion Test

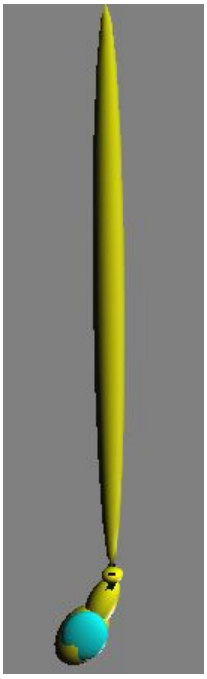

Figure 51. Neck Lateral Flexion Test at Peak Angle

The following graphs show the comparison of the pendulum acceleration, moment at O.C. (in Y direction), and the force in the X direction obtained for the model without spring dampers and run using the ATBV3 program (Figure 52, 53, & 54).

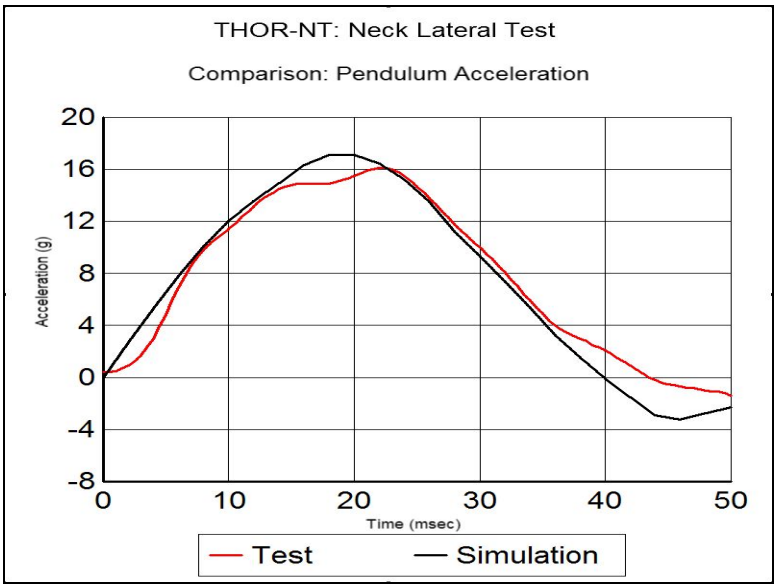

Figure 52. Comparison of Test and Simulation Pendulum Acceleration for Neck Lateral Flexion Test

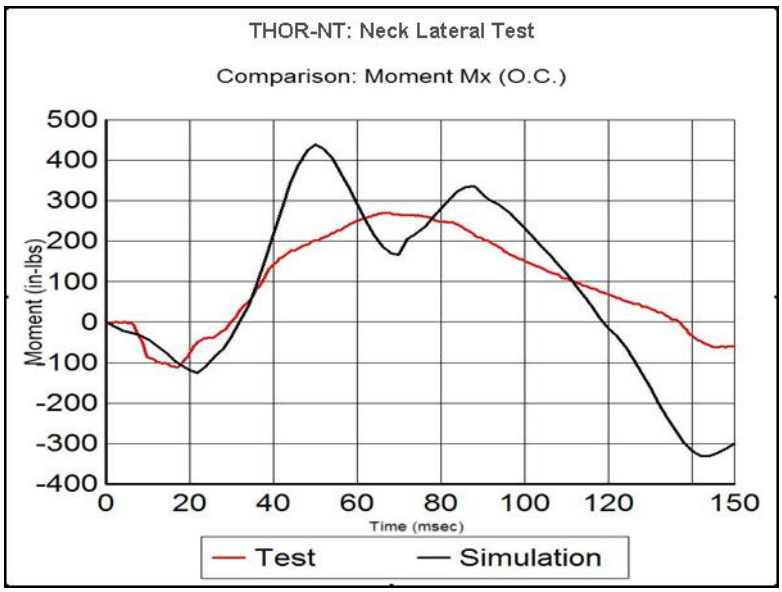

Figure 53. Comparison of Test and Simulation Mx at O.C. for Neck Lateral Test (without Spring/Cable Model)

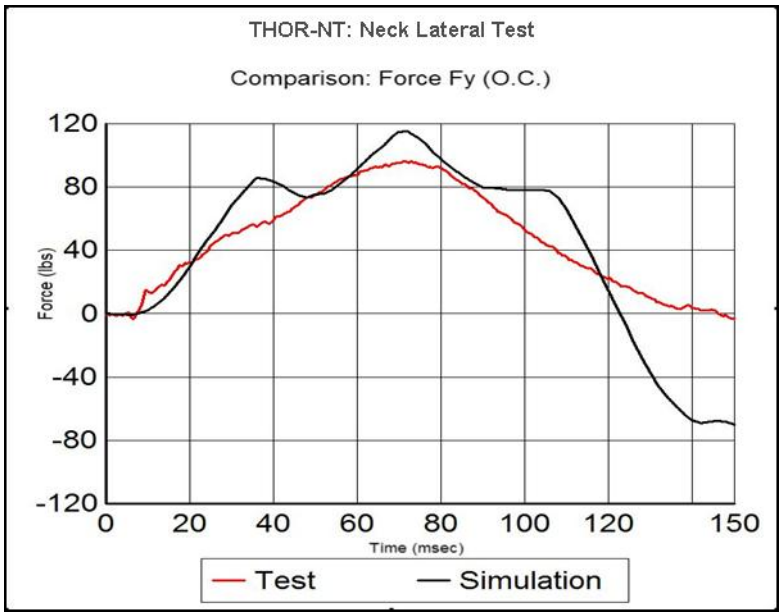

Figure 54. Comparison of Test and Simulation Fy at O.C. for Neck Lateral Test (without Spring/Cable Model)

The figures above show that the acceleration profile for the lateral flexion is reproduced well (Figure 52). There is not a good match of the main peak of the Mx response (Figure 53) and the simulation shows two peaks, though the general, average shape does match the test curve. The shear force, Fy, also shows the same general shape as the test, but shows oscillations that are not seen in the test (Figure 54).

The following show the results from the model with the spring/dampers using DYNAMAN. The neck springs are not significantly engaged for the lateral test (Figures 55 & 56).

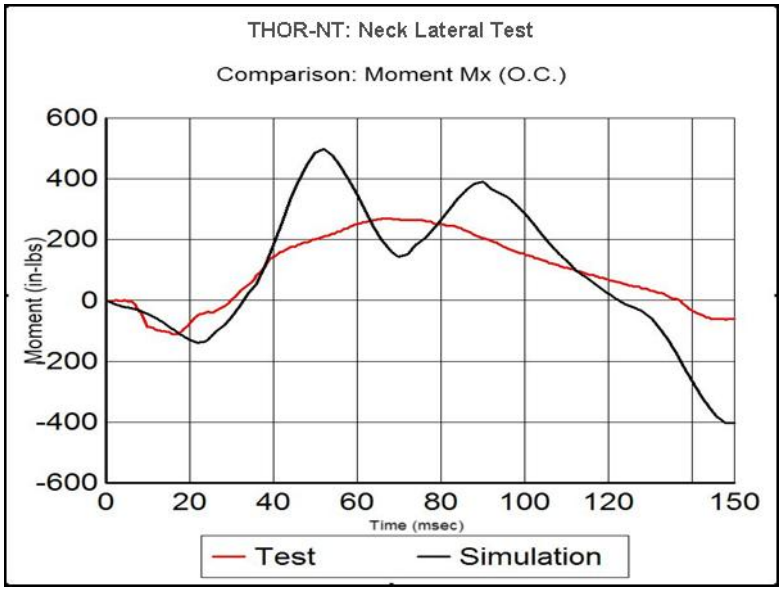

Figure 55. Comparison of Test and Simulation Mx at O.C. for Neck Lateral Test (with Spring/Cable Model)

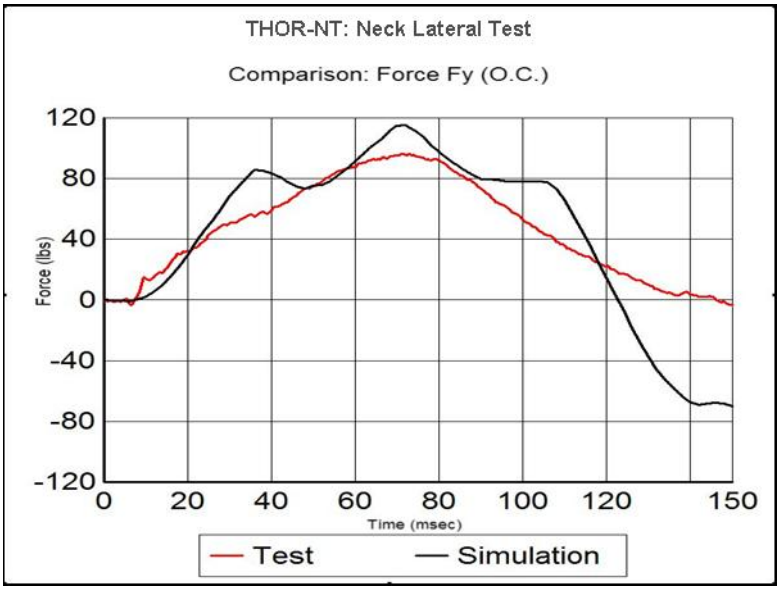

Figure 56. Comparison of Test and Simulation Fy at O.C. for Neck Lateral Test (with Spring/Cable Model)

It is seen that there is no significant change in going from the model without spring/dampers to the model with them (Figures 55 & 56). This is not surprising, since the springs do not play a role during lateral flexion.

Overall, it is seen that the model with spring/dampers has a somewhat better reproduction of the test results than without these elements. But the model without spring/dampers should be adequate for general whole-body simulations.

3.10. THOR-NT Simulation Input Data Sets for ATB V.3 Program

The following are the input files (*.LIN format) for the various simulations that were carried out while modeling the NT certification tests. Please note that there may have been some discrepancies for most of the above certification test results between DYNAMAN and ATB V.3 due to the different versions of ATB program used in the back-end solvers.

Whole body tests:

These input files use the whole THOR model. Only the impactor description changes as well as the segment/ellipsoid that is contacted. The segment orientations are the same for all tests except for the femur/knee impact (where the dummy is in a sitting position), and for the head impact, where the head is tilted forward to allow impact to forehead.

ntfcdsk - face disk impact
ntfcrod - face rod impact
nthdimp - head impact with disk
ntfemur - knee impact with disk
ntkr43 - sternal impact at 4.3 m/s (low-speed Kroell test)

ntkr67 - sternal impact at 6.7 m/s (high-speed Kroell test)
ntloabd - lower abdomen impact with rod
ntmcw - lower ribcage oblique impact with disk
ntupabd - upper abdomen impact with steering wheel

Component tests:

LX (includes only upper tibia, lower tibia, and foot):

ntlxheel - impact to heel of foot
ntlxball - impact to ball of foot (with tibia joint locked)

Neck (includes only head and neck attached to pendulum arm):

ntnkflx - pendulum impact in frontal flexion
ntnkext - pendulum impact in extension
ntnklat - pendulum impact in lateral flexion

3.11. THOR-NT Sled Model ATB Simulation

A basic sled model, with shoulder and lap belts, was developed (Figure 57). Only a generic seat and floor were defined. The THOR-NT model used in all the whole-body certification tests was used. Contacts of the upper body and upper legs with the seat cushion and seat back were modeled. A shoulder ellipsoid was added for proper contact with the shoulder belt, and contact between the left and right upper femurs and lower femurs were defined (ellipsoid-ellipsoid contacts).

A generic sled pulse with peak acceleration of 25g and delta-V of 25 mph was defined. The basic objective was to evaluate the motion of the dummy in the model to determine if any unrealistic motions are observed (Figure 58).

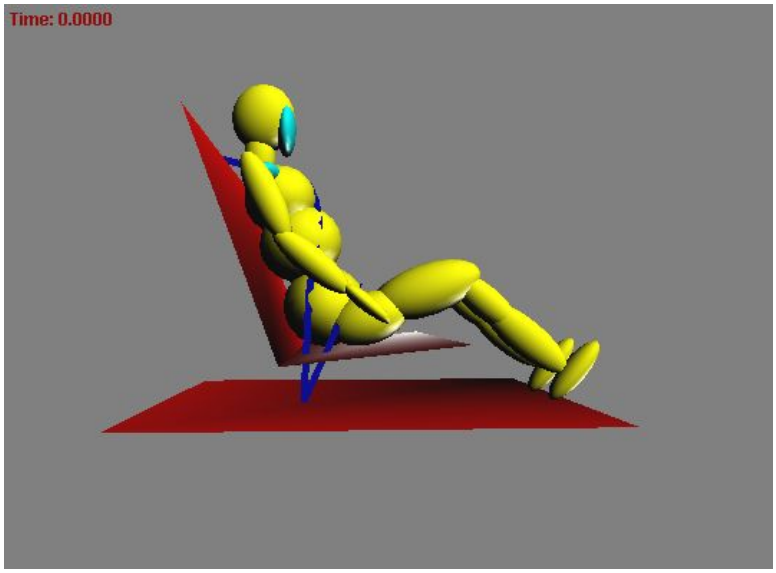

Figure 57. Initial Setup of THOR-NT in Generic Sled

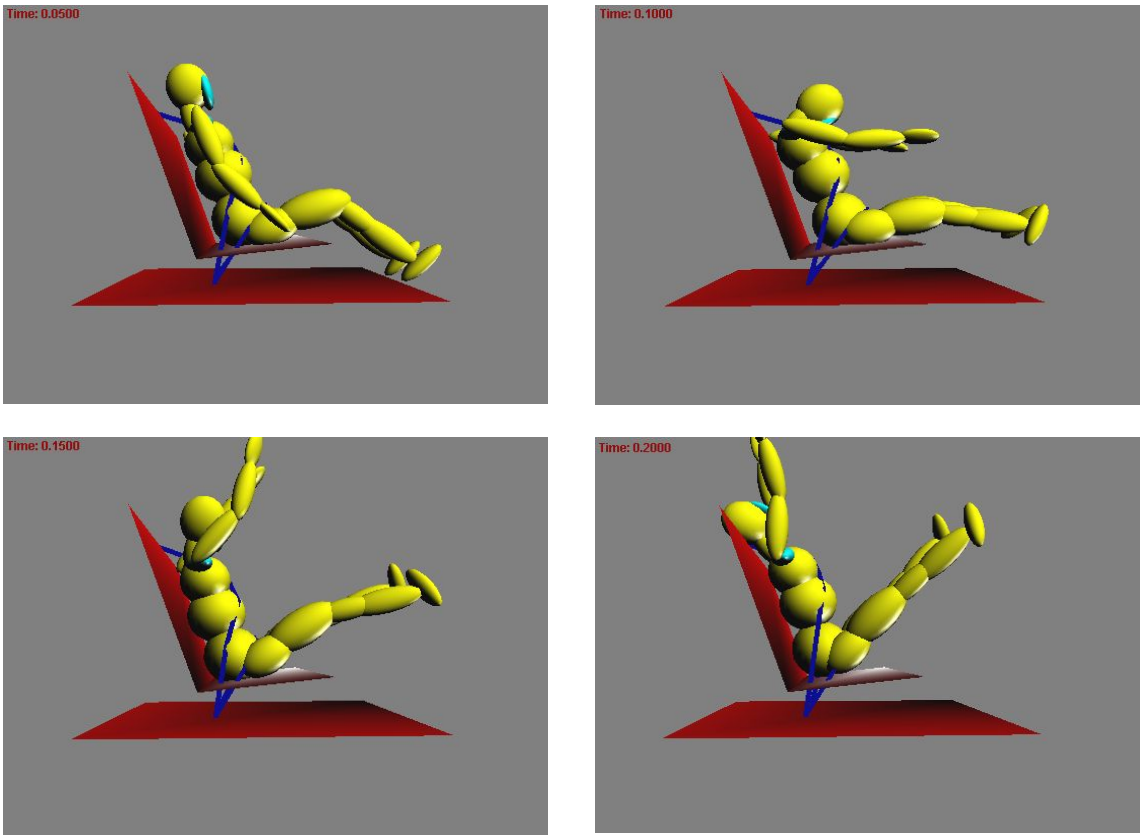

Figure 58. Four Frames of Full Body Sled Simulation at 50 msec Intervals

4. MODIFICATION OF GEBOD PROGRAM FOR ADDITION OF THOR-NT DUMMY

The GEBOD program has been used to generate body data sets for ATB simulations. It has options for both human and manikin data sets. The human data sets are based largely on a set of regression equations from anthropometric survey. The dummy data sets are based on direct measurements. GEBOD places these measurement values in the data file GEBOD.DAT. It reads them directly from GEBOD.DAT and outputs them in ATB input format. Currently, GEBOD has data sets of 50 percentile sitting and standing Hybrid II and Hybrid III dummies. It also has a sitting Hybrid III dummy with enhanced lower extremity model (Pellettiere, *et al.*, 1998).

To facilitate the use of THOR-NT with the ATB program, AFRL has added a sitting THOR-NT data set into the GEBOD program. The data are directly from the THOR-NT sled simulation discussed in section 3.11. The cards of B, D.1, D.5, E.1, and E.7 of the sled simulation input file were appended to the GEBOD.DAT file. Among these cards, cards E.1 are force-deflection functions that are not usually produced by GEBOD. The reason to include them for THOR-NT dummy is that there are some functions used to describe THOR-NT's deformable characteristics. However since these contact properties are related to the contact surface, care must be taken before using them for other different simulations. Cards D.5 include two additional contact ellipsoids, Ellipsoid No. 23 and Ellipsoid No. 24, representing the face disk and clavicle respectively. They are used for face and belt contacts. Cards D.5 define only their sizes without information on which segments they are attached to. Users need to define their corresponding segment attachment in the contact definition portion of the ATB input file.

The modified GEBOD functions are:

CRESULTS:

1. Added new option of dummy choice '9' which corresponds to 'THOR-NT' dummy.
2. Output format variable now accepts '1','2',or '3' for input. This corresponds to what kind of output is desired: (ain, lin, tabular). Note: only for THOR-NT dummy.

The newly created GEBOD functions are:

ATBAINOUT:

Reads data from GEBOD.DAT file. Outputs B cards, E cards, D.5 card, and F.4 card in both ain and tabular formats. Function only used for THOR-NT dummy. Both metric and English datasets supported.

NOATBLINOUT:

Reads data from GEBOD file. Outputs B cards, E cards, D.5 card, and F.4 card in only tabular format. Function only used for THOR-NT dummy. Both metric and English datasets supported.

ATBLINOUT:

Reads data from GEBOD.DAT file. Outputs B cards, E cards, D.5 card, and F.4 card in both lin and tabular formats. Function only used for THOR-NT dummy. Both metric and English datasets supported.

5. CONCLUSION

THOR-NT has many enhancements compared to the previous generation of dummies. The ATB model of THOR-NT dummy offers its users a low cost and quick simulation tool. Compared with the 17 segment Hybrid III ATB dummy model, ATB THOR-NT model has 21 segments with extra 4 segments to model two-part tibia and femur. They allow the incorporation of a slip joint between the two parts. Additional ellipsoids such as face disk and clavicle were added with contact properties to model deformable face and shoulder belt contact. Efforts were also made to model the neck's five rubber pucks but the results were not practical when used in general simulations with free neck rotions in all directions.

Mass properties such as weight, moments of inertia, and principal axes were measured with respect to the segment local reference systems through a set of skeletal landmarks. A set of force-deflection and damping functions were derived through dynamic impact test results and represent the deformable characteristics of the segments. Joint stiffness functions were developed from quasi-static and dynamic tests. Contact ellipsoid dimensions were made from CAD drawings.

The GEBOD program was modified to add the THOR-NT ATB data set as a new dummy option. It produces corresponding ATB input cards related to the dummy, including force-deflection functions. A set of ATB simulations were developed to model component certification tests for comparison and validation. Some observations on the simulation results and test responses show:

1. The simulations reproduce the general shapes of test responses for most cases.
2. The peak values of simulation results approximate relatively well to the test responses for most cases.
3. There are some discrepancies on the rise and unloading profiles for some cases due to the limitation of lumped mass model.
4. There are discrepancies on both the shapes and peak values between some neck simulations and tests. Average shapes are reproduced though there are several unwanted small peaks in the results. The difference in the peak values between the simulations and tests are within 30% of the test values. These discrepancies are due to the limitation of applying a rigid ATB neck model to the flexible multi-plate dummy neck.

A generic THOR-NT sled simulation was also performed and the movements of the dummy seem reasonable. A new ATB THOR-NT simulation on a certification sled test is under progress.

Overall, the ATB model of the THOR-NT dummy reproduces the dummy's kinematic and dynamic responses relatively well, compared to the performance of other ATB dummy models as well as ATB model's own limitation. Some addition work may yield a neck model that represents the THOR-NT neck more accurately. When used properly, ATB model can serve as an effective preliminary assessment tool for studies involving THOR-NT dummy.

6. REFERENCES

Cheng, H., Obergefell, L., and Rizer, A., 1994, "Generator of Body Data (GEBOD) Manual", AL/CF-TR-1994-0051, Air Force Research Laboratory, Human Effectiveness Directorate, Bioscience and Protection Division, 2800 Q Street, Wright-Patterson AFB OH 45433-7947.

Cheng, H., Rizer, A., and Obergefell, L., 1998, "Articulated Total Body Model Version V User's Manual", AFRL-HE-WP-TR-1998-0015, Air Force Research Laboratory, Human Effectiveness Directorate, Bioscience and Protection Division, 2800 Q Street, Wright-Patterson AFB OH 45433-7947.

Fleck, J. and Butler, F., 1982, "Validation of the Crash Victim Simulator; Volume 3: User's Manual", Department of Transportation Report No. DTO-HS-806-281.

Fleck, J. and Butler, F., 1982, "Validation of the Crash Victim Simulator; Volume 4: Programmer's Manual", Department of Transportation Report No. DOT-HS-806-282.

Gardner, T., 2004, "Upgrading the ATB Model Code from FORTRAN 77 to FORTRAN 90", AFRL-HE-WP-TR-2004-0113, Air Force Research Laboratory, Human Effectiveness Directorate, Bioscience and Protection Division, 2800 Q Street, Wright-Patterson AFB OH 45433-7947.

GESAC, Inc., 2005, "THOR-NT User's Manual", GESAC Report No. GESAC-05-02, General Engineering and Systems Analysis Company, Inc, 125 Orchard Drive, Boonsboro, MD 21713.

Gross, M., 1991, "The GOBODIII Program User's Guide and Description", AL-TR-1991-0102, Air Force Research Laboratory, Human Effectiveness Directorate, Bioscience and Protection Division, 2800 Q Street, Wright-Patterson AFB OH 45433-7947.

Obergefell, L., Fleck, J., Kaleps, I., and Gardner, T., 1988, "Articulated Total Body Model Enhancements, Volume 3: Programmer's Guide", AAMRL-TR-88-009, Air Force Research Laboratory, Human Effectiveness Directorate, Bioscience and Protection Division, 2800 Q Street, Wright-Patterson AFB OH 45433-7947.

Pellettiere, J., Sieveka, E., Crandall, J., Pilkey, W., Tanahashi, M., Weisenfeld, G., Okuhara, H., Takahashi, Y., and Okamoto, Y., 1998, "Experimental Testing of the Hybrid III Lower Extremity for Computational Model Development", SAE Paper 980363, International Congress & Exposition, February 1998, Detroit, MI, USA.

APPENDIX A

A.1. Portion of the Output File of ATB Generic THOR-NT Sled Simulation

The following is the first part of the ATB primary output file for the generic THOR-NT sled simulation as described in section 3.11 of this report. It lists all the ATB simulation input cards in tabular format with all the variables clearly labeled. Cards B, D.5, E.1 ~E.4, and E.7 are THOR-NT dummy data. Refer to Articulated Total Body Model Version V User's Manual (Cheng, Rizer, & Obergefell, 1998) for more information on the ATB input cards and simulation setup.

Developed by CALSPAN Corp., P.O. Box 400, Buffalo NY 14225
and by J&J Technologies Inc., Orchard Park, NY 14127

For the Armstrong Aerospace Medical Research Laboratory
Wright-Patterson Air Force Base
Under contracts F33615-75C-5002,-78C-0516 and -80C-05117

and for the National Highway Traffic Safety Administration,
U.S. Department of Transportation, under contracts
FH-11-7592, HS-053-2-485, HS-6-01300 and HS-6-01410,

Modified by GESAC, Inc. to incorporate water forces,
by Armstrong Lab. for robotic motion simulation,
and finite element models of deformable segments,
and by BlackRock Dynamics, Inc. to convert the
code to Fortran 90/95.

Program documentation: NHTSA Report Nos. DOT-HS-801-507
through 510 (formerly CALSPAN Report No. ZQ-5180-L-1),
Available from NTIS (accession nos. PB-241692,3,4 and 5),
Appendixes A-J to the above (Available from CALSPAN),
and report nos. AMRL-TR-75-14 (NTIS NO. AD-A014 816),
AFAMRL-TR-80-14 (NTIS NO. AD-A088 029), and
AFAMRL-TR-83-073 (NTIS NO. AD-B079 184).

The most recent documentation is in report nos.
AFRL-HE-WP-TR-1998-0015.
PROGRAM ATB Version 5.3.1 (July 10, 2004)

The Government makes no express or implied
warranty as to any matter whatsoever including the
conditions of the research or any product agreement
or of the merchantability, validity, suitability,
or fitness for a particular
purpose of the research or product developed from
the use of this software. In no event will the
Government be liable to any other party for
compensatory, punitive, exemplary or consequential
damages. The Government is neither liable nor
responsible for maintenance, updating or correcting
any errors in the provided software. The user
accepts all risks and responsibilities from the
following analysis. Please see the ATB Users

guide for information on suppressing this startup
message in the future. The user has accepted these
terms by executing the following analysis

08/10/2006 Cards A

Data Set for THOR NT
General Setup for Sled

UNITL = IN UNITM = LBS UNITT = SEC Gravity Vector = (0.0000, 0.0000, 386.1000) G = 386.1000

NDINT = 6 NSTEPS = 40 DT =0.005000 H0 =0.001000 HMAX =0.001000 HMIN =0.000063

0 NPRT Array

1	2	3	4	5	6	7	8	9	10	11	12	13	14	15	16	17	18	19	20	21	22	23	24	25	26	27	28	29	30	31	32	33	34	35	36
1	0	10	2	0	0	0	0	0	0	0	0	0	0	0	0	0	0	0	0	0	0	0	0	0	0	0	0	0	0	0	0	0	0	0	1

1 Test Subject THOR-NT 21 Segments 20 Joints

Card B.1
Cards B.2

Segment I	SYM	Weight (LBS)	Principal Moments of Inertia (LBS-SEC**2-IN) X	Y	Z	Segment Contact Ellipsoid Semiaxes (IN) X	Y	Z	Center (IN) X	Y	Z	Principal Axes (DEG) Yaw	Pitch	Roll
1	pelv	33.600	1.2860	0.8900	0.9480	5.250	7.200	5.250	0.500	0.000	-0.750	0.00	37.00	180.00
2	lthx	21.910	0.6040	0.5890	0.4830	5.250	6.000	5.000	0.450	0.000	-2.400	0.00	0.00	180.00
3	uthx	29.590	1.4140	1.2950	0.6310	4.500	5.500	4.500	0.600	0.000	1.450	0.00	-25.00	180.00
4	nk	3.640	0.0430	0.0430	0.0070	2.000	2.000	4.000	-0.100	0.000	0.600	0.00	0.00	180.00
5	hd	10.160	0.1870	0.2030	0.1130	4.000	3.125	4.500	-0.355	0.000	0.000	0.00	37.00	180.00
6	rulu	6.770	0.1440	0.1230	0.0480	3.250	3.250	5.000	-1.000	0.250	0.800	0.00	0.00	180.00
7	rull	9.810	0.2910	0.2670	0.0770	3.250	3.250	7.000	0.300	-0.100	-1.400	0.00	0.00	180.00
8	rllu	3.970	0.0700	0.0690	0.0150	2.000	1.800	5.500	-0.100	0.000	0.000	0.00	0.00	180.00
9	rlll	4.410	0.0920	0.0970	0.0150	2.250	1.750	6.500	-0.200	0.150	-1.200	0.00	0.00	180.00
10	rf	2.090	0.0240	0.0470	0.0460	4.700	1.800	1.500	-0.700	0.000	0.000	-15.00	6.00	-161.00
11	lulu	6.770	0.1440	0.1230	0.0480	3.250	3.250	5.000	-1.000	-0.250	0.800	0.00	0.00	180.00
12	lull	9.810	0.2910	0.2670	0.0770	3.250	3.250	7.000	0.300	0.100	-1.400	0.00	0.00	180.00
13	lllu	3.970	0.0700	0.0690	0.0150	2.250	1.750	5.500	-0.100	0.000	0.000	0.00	0.00	180.00
14	llll	4.410	0.0920	0.0970	0.0150	2.250	1.750	6.500	-0.200	-0.150	-1.200	0.00	0.00	180.00
15	lf	2.090	0.0240	0.0470	0.0460	4.700	1.800	1.500	-0.700	0.000	0.000	-15.00	-6.00	161.00
16	rua	4.597	0.1024	0.0997	0.0109	1.900	1.800	6.000	0.000	0.000	-1.000	0.00	-1.31	180.00
17	rla	3.800	0.1191	0.1128	0.0069	1.775	1.775	5.800	0.000	0.000	0.000	0.00	-1.31	180.00
18	rhd	1.290	0.0114	0.0093	0.0036	1.000	1.870	3.650	0.000	0.000	0.000	-5.35	30.75	173.50
19	lua	4.597	0.1024	0.0997	0.0109	1.900	1.800	6.000	0.000	0.000	-1.000	0.00	-1.31	180.00
20	lla	3.800	0.1191	0.1128	0.0069	1.775	1.775	5.800	0.000	0.000	0.000	0.00	-1.31	180.00
21	lhd	1.290	0.0114	0.0093	0.0036	1.000	1.870	3.650	0.000	0.000	0.000	5.35	30.75	-173.50

Cards B.3

Joint J	SYM	JNT	FIN	Location(IN) - Seg(JNT) X	Y	Z	Location(IN) - Seg(J+1) X	Y	Z	Joint Axis(deg) - Seg(JNT) ID1 Yaw	ID2 Pitch	ID3 Roll	Joint Axis(deg) - Seg(J+1) ID4 Yaw	ID5 Pitch	ID6 Roll

1	lumb	1	0	-1.540	0.000	-4.420	-1.300	0.000	2.350	3	0.00	2	0.00	1	0.00	3	0.00	2	0.00	1	0.00
2	thx	2	0	-1.900	0.000	-6.950	-1.450	0.000	3.250	3	0.00	2	0.00	1	0.00	3	0.00	2	0.00	1	0.00
3	np	3	0	-0.850	0.000	-1.430	0.100	0.000	4.000	3	0.00	2	0.00	1	0.00	3	0.00	2	0.00	1	0.00
4	oc	4	0	0.100	0.000	-2.630	-0.640	0.000	1.960	3	0.00	2	0.00	1	0.00	3	0.00	2	0.00	1	0.00
5	rh	1	2	0.950	3.290	1.500	0.000	-1.200	-3.500	3	0.00	2	90.00	1	0.00	3	0.00	2	0.00	1	0.00
6	rfm	6	-6	-0.100	0.200	2.800	0.300	-0.100	-7.250	3	0.00	2	0.00	1	0.00	3	0.00	2	0.00	1	0.00
7	rk	7	1	0.300	-0.100	2.700	0.000	-0.150	-4.200	3	0.00	2	0.00	1	0.00	3	0.00	2	55.00	1	0.00
8	rtb	8	-6	-0.100	0.000	2.800	0.000	0.150	-5.300	3	0.00	2	0.00	1	0.00	3	0.00	2	0.00	1	0.00
9	ra	9	0	0.100	0.150	4.700	-1.100	0.000	-1.450	3	0.00	2	0.00	1	0.00	3	0.00	2	0.00	1	0.00
10	lh	1	2	0.950	-3.290	1.500	0.000	1.200	-3.500	3	0.00	2	90.00	1	0.00	3	0.00	2	0.00	1	0.00
11	lfm	11	-6	-0.100	-0.200	2.800	0.300	0.100	-7.250	3	0.00	2	0.00	1	0.00	3	0.00	2	0.00	1	0.00
12	lk	12	1	0.300	0.100	2.700	0.000	0.150	-4.200	3	0.00	2	0.00	1	0.00	3	0.00	2	55.00	1	0.00
13	ltb	13	-6	-0.100	0.000	2.800	0.000	-0.150	-5.300	3	0.00	2	0.00	1	0.00	3	0.00	2	0.00	1	0.00
14	la	14	0	0.100	-0.150	4.700	-1.100	0.000	-1.450	3	0.00	2	0.00	1	0.00	3	0.00	2	0.00	1	0.00
15	rs	3	0	-0.880	7.380	-2.660	0.000	0.000	-5.430	3	0.00	2	90.00	1	0.00	3	0.00	2	0.00	1	0.00
16	re	16	-8	0.000	0.000	4.940	0.000	0.000	-3.670	3	90.00	2	0.00	1	0.00	3	90.00	2	0.00	1	0.00
17	rw	17	-8	0.000	0.000	6.070	-0.300	0.000	-2.130	3	90.00	2	0.00	1	0.00	3	90.00	2	0.00	1	0.00
18	ls	3	0	-0.880	-7.380	-2.660	0.000	0.000	-5.430	3	0.00	2	90.00	1	0.00	3	0.00	2	0.00	1	0.00
19	le	19	-8	0.000	0.000	4.940	0.000	0.000	-3.670	3	90.00	2	0.00	1	0.00	3	90.00	2	0.00	1	0.00
20	lw	20	-8	0.000	0.000	6.070	-0.300	0.000	-2.130	3	90.00	2	0.00	1	0.00	3	90.00	2	0.00	1	0.00

Unlock Conditions for Slip Joints

Joint	Tension (LBS)	Compression (LBS)
6	0.000	0.000
8	0.000	0.000
11	0.000	0.000
13	0.000	0.000

1 Joint Torque Characteristics

Flexural Spring Characteristics

Joint	Spring Coef. (IN LBS /deg**J) Linear (J=1)	Quadratic (J=2)	Cubic (J=3)	Energy Dissipation Coef.	Joint Stop (deg)
1 lumb	-81.000	0.000	0.000	0.000	0.000
2 thx	-82.000	0.000	0.000	0.000	0.000
3 np	-83.000	0.000	0.000	0.000	0.000
4 oc	-84.000	0.000	0.000	0.000	0.000
5 rh	-87.000	0.000	0.000	0.000	0.000
6 rfm	0.000	0.000	0.000	1.000	0.000
7 rk	0.000	2.320	0.000	1.000	48.900
8 rtb	0.000	0.000	0.000	1.000	0.000
9 ra	-89.000	0.000	0.000	0.000	0.000
10 lh	-88.000	0.000	0.000	0.000	0.000
11 lfm	0.000	0.000	0.000	1.000	0.000
12 lk	0.000	2.320	0.000	1.000	48.900

Torsional Spring Characteristics

Joint	Spring Coef. (IN LBS /deg**J) Linear (J=1)	Quadratic (J=2)	Cubic (J=3)	Energy Dissipation Coef.	Joint Stop (deg)
1 lumb	34.000	0.000	0.000	1.000	0.000
2 thx	34.000	0.000	0.000	1.000	0.000
3 np	8.000	0.000	0.000	1.000	0.000
4 oc	8.000	0.000	0.000	1.000	0.000
5 rh	7.500	75.000	75.000	1.000	55.000
6 rfm	0.000	0.000	0.000	1.000	0.000
7 rk	0.000	0.000	0.000	1.000	0.000
8 rtb	0.000	0.000	0.000	1.000	0.000
9 ra	-90.000	0.000	0.000	0.000	0.000
10 lh	7.500	75.000	75.000	1.000	55.000
11 lfm	0.000	0.000	0.000	1.000	0.000
12 lk	0.000	0.000	0.000	1.000	0.000

13	ltb	0.000	0.000	0.000	1.000	0.000	0.000	0.000	0.000	1.000	0.000
14	la	-89.000	0.000	0.000	0.000	0.000	-90.000	0.000	0.000	0.000	0.000
15	rs	-85.000	0.000	0.000	0.000	0.000	0.000	100.000	100.000	1.000	125.000
16	re	0.000	20.000	20.000	1.000	52.000	0.000	4.650	0.000	1.000	65.300
		0.000	0.000	0.000	1.000	0.000					
17	rw	0.000	0.000	0.000	1.000	0.000	0.000	4.320	0.143	1.000	55.500
		0.000	0.000	0.000	1.000	0.000					
18	ls	-86.000	0.000	0.000	0.000	0.000	0.000	100.000	100.000	1.000	125.000
19	le	0.000	20.000	20.000	1.000	52.000	0.000	4.650	0.000	1.000	65.300
		0.000	0.000	0.000	1.000	0.000					
20	lw	0.000	0.000	0.000	1.000	0.000	0.000	4.320	0.143	1.000	55.500
		0.000	0.000	0.000	1.000	0.000					

Cards B.5

Joint Viscous Characteristics and Lock-Unlock Conditions

Joint	Viscous Coefficient (IN LBS SEC /DEG)	Coulomb Friction Coef. (IN LBS)	Full Friction Angular Velocity (DEG/SEC)	Max Torque for a Locked Joint (IN LBS)	Min Torque for Unlocked Joint (IN LBS)	Min. Ang. Velocity for Unlocked Joint (RAD/SEC)	Impulse Restitution Coefficient
1 lumb	0.000	0.00	30.00	0.00	0.00	0.00	0.000
2 rhx	0.000	0.00	30.00	0.00	0.00	0.00	0.000
3 np	0.020	0.00	30.00	0.00	0.00	0.00	0.000
4 oc	0.020	20.00	30.00	0.00	0.00	0.00	0.000
5 rh	0.000	0.00	30.00	0.00	0.00	0.00	0.000
6 rfm	0.000	0.00	30.00	0.00	0.00	0.00	0.000
7 rk	0.000	0.00	30.00	0.00	0.00	0.00	0.000
8 rtb	0.000	0.00	30.00	0.00	0.00	0.00	0.000
9 ra	0.030	0.00	30.00	0.00	0.00	0.00	0.000
10 lh	0.000	0.00	30.00	0.00	0.00	0.00	0.000
11 lfm	0.000	0.00	30.00	0.00	0.00	0.00	0.000
12 lk	0.000	0.00	30.00	0.00	0.00	0.00	0.000
13 ltb	0.000	0.00	30.00	0.00	0.00	0.00	0.000
14 la	0.030	0.00	30.00	0.00	0.00	0.00	0.000
15 rs	0.000	0.00	30.00	0.00	0.00	0.00	0.000
16 re	0.100	0.00	30.00	0.00	0.00	0.00	0.000
	0.100	0.00	30.00	0.00	0.00	0.00	0.000
	0.000	0.00	30.00	0.00	0.00	0.00	0.000
17 rw	0.500	0.00	30.00	0.00	0.00	0.00	0.000
	0.500	0.00	30.00	0.00	0.00	0.00	0.000
	0.000	0.00	30.00	0.00	0.00	0.00	0.000
18 ls	0.000	0.00	30.00	0.00	0.00	0.00	0.000
19 le	0.100	0.00	30.00	0.00	0.00	0.00	0.000
	0.100	0.00	30.00	0.00	0.00	0.00	0.000
	0.000	0.00	30.00	0.00	0.00	0.00	0.000
20 lw	0.500	0.00	30.00	0.00	0.00	0.00	0.000
	0.500	0.00	30.00	0.00	0.00	0.00	0.000
	0.000	0.00	30.00	0.00	0.00	0.00	0.000

1

Segment Integration Convergence Test Input

Cards B.6

Segment No.	Sym	Angular Velocities (rad/SEC) Mag. Test	Abs. Error	Rel. Error	Linear Velocities (IN /SEC) Mag. Test	Abs. Error	Rel. Error	Angular Accelerations (rad/SEC **2) Mag. Test	Abs. Error	Rel. Error	Linear Accelerations (IN /SEC **2) Mag. Test	Abs. Error	Rel. Error
1	pelv	0.000	0.000	0.0000	0.000	0.000	0.0000	0.010	0.010	0.0100	0.001	0.001	0.0010
2	lthx	0.000	0.000	0.0000	0.000	0.000	0.0000	0.010	0.010	0.0100	0.000	0.000	0.0000
3	uthx	0.000	0.000	0.0000	0.000	0.000	0.0000	0.010	0.010	0.0100	0.000	0.000	0.0000
4	nk	0.000	0.000	0.0000	0.000	0.000	0.0000	0.010	0.010	0.0100	0.000	0.000	0.0000
5	hd	0.000	0.000	0.0000	0.000	0.000	0.0000	0.010	0.010	0.0100	0.000	0.000	0.0000
6	rulu	0.000	0.000	0.0000	0.000	0.000	0.0000	0.010	0.010	0.0100	0.000	0.000	0.0000
7	rull	0.000	0.000	0.0000	0.000	0.000	0.0000	0.010	0.010	0.0100	0.000	0.000	0.0000
8	rllu	0.000	0.000	0.0000	0.000	0.000	0.0000	0.010	0.010	0.0100	0.000	0.000	0.0000
9	rlll	0.000	0.000	0.0000	0.000	0.000	0.0000	0.010	0.010	0.0100	0.000	0.000	0.0000
10	rf	0.000	0.000	0.0000	0.000	0.000	0.0000	0.010	0.010	0.0100	0.000	0.000	0.0000
11	lulu	0.000	0.000	0.0000	0.000	0.000	0.0000	0.010	0.010	0.0100	0.000	0.000	0.0000
12	lull	0.000	0.000	0.0000	0.000	0.000	0.0000	0.010	0.010	0.0100	0.000	0.000	0.0000
13	lllu	0.000	0.000	0.0000	0.000	0.000	0.0000	0.010	0.010	0.0100	0.000	0.000	0.0000
14	llll	0.000	0.000	0.0000	0.000	0.000	0.0000	0.010	0.010	0.0100	0.000	0.000	0.0000
15	lf	0.000	0.000	0.0000	0.000	0.000	0.0000	0.010	0.010	0.0100	0.000	0.000	0.0000
16	rua	0.000	0.000	0.0000	0.000	0.000	0.0000	0.010	0.010	0.0100	0.000	0.000	0.0000
17	rla	0.000	0.000	0.0000	0.000	0.000	0.0000	0.010	0.010	0.0100	0.000	0.000	0.0000
18	rhd	0.000	0.000	0.0000	0.000	0.000	0.0000	0.010	0.010	0.0100	0.000	0.000	0.0000
19	lua	0.000	0.000	0.0000	0.000	0.000	0.0000	0.010	0.010	0.0100	0.000	0.000	0.0000
20	lla	0.000	0.000	0.0000	0.000	0.000	0.0000	0.010	0.010	0.0100	0.000	0.000	0.0000
21	lhd	0.000	0.000	0.0000	0.000	0.000	0.0000	0.010	0.010	0.0100	0.000	0.000	0.0000

1 Vehicle Deceleration Inputs

Cards C

Vehicle Motion

Yaw	Pitch	Roll	VIPS	VTIME	X0(X)	X0(Y)	X0(Z)	NATAB	AT0	ADT	I1	I3	MSEG
0.000	0.000	0.000	0.000	0.000	0.000	0.000	0.000	15	0.00000	0.01000	0	0	0

0 Unidirectional Vehicle Position Tables

Time (msec)	Acc (G)	Velocity (IN /SEC)	Position (IN)	Time (msec)	Acc (G)	Velocity (IN /SEC)	Position (IN)
0.00000	0.00	0.0000	0.00000				
10.00000	2.00	-3.2175	-0.00643				
20.00000	6.00	-18.0180	-0.10296				
30.00000	14.00	-56.6280	-0.45045				
40.00000	22.00	-126.1260	-1.33848				
50.00000	21.00	-209.7810	-3.02445				
60.00000	18.00	-285.7140	-5.50836				
70.00000	13.00	-344.9160	-8.67438				
80.00000	10.00	-388.6740	-12.35520				
90.00000	6.00	-419.5620	-16.40925				
100.00000	2.00	-435.0060	-20.69496				
110.00000	1.00	-440.7975	-25.07720				

```
  120.00000       0.00     -442.7280     -29.49804
  130.00000       0.00     -442.7280     -33.92532
  140.00000       0.00     -442.7280     -38.35260
1  Vehicle Paths to Ground                                                                                    Page     6

 The ground (inertial) segment is represented here by a 0.
 The coord category refers to the coordinate system in which the vehicle data are specified.
 A negative value for coord indicates that the data represent accelerometer data.

    Veh  Coord    Vehicle Path to Ground
    VEH   GRND    GRND
      22     0       0

1    NPL    NBLT    NBAG    NELP      NQ     NSD  NHRNSS  NWINDF  NJNTFOLD  NFORCE   NWATER   NEXTCD                  Page     7
       3       0       0       2       0       4       1       0         0       0        0        0                Card D.1a
0 Plane Inputs                                                                                                     Cards D.2
0 Plane No.   1    seat

                 X           Y           Z
  Point 1     -34.0000    -25.0000     -6.0000
  Point 2     -34.0000     25.0000     -6.0000
  Point 3     -16.0000    -25.0000     -8.0000
0 Plane No.   2    seat

                 X           Y           Z
  Point 1     -34.0000    -25.0000     -6.0000
  Point 2     -43.0000    -25.0000    -31.0000
  Point 3     -34.0000     25.0000     -6.0000
0 Plane No.   3    floor

                 X           Y           Z
  Point 1     -50.0000    -25.0000      0.0000
  Point 2     -50.0000     25.0000      0.0000
  Point 3       0.0000    -25.0000      0.0000
1 Additional Ellipsoid Input                                                                                   Page     8
                                                                                                             Cards D.5
                Semiaxes (IN  )              Offset (IN  )              Rotation (deg)                Power
   No.        X         Y         Z          X         Y         Z          Yaw       Pitch      Roll

    23       1.250     3.000     3.500       2.500     0.000     1.500      0.000     0.000     0.000      0.    0.    0.
    24       2.250     8.000     1.800       0.000     0.000    -1.500      0.000     0.000     0.000      0.    0.    0.
0 Body Segment Symmetry Input                                                                                  Card D.7

  Seg No.   1   2   3   4   5   6   7   8   9  10  11  12  13  14  15  16  17  18  19  20  21
0 NSYM(J)   0   0   0   0   0   0   0   0   0   0   0   0   0   0   0   0   0   0   0   0   0
0     Spring  Dampers  Function  Input                                                                          Cards D.8

                Coordinates of Attachment Points (IN  )
     Segment         Segment M                Segment N            Spring Force Function          Damping Force Function
 No.  M   N      X         Y         Z        X         Y         Z        D0          A1          A2          B1          B2
```

1	6	7	0.00	0.00	3.00	0.00	0.00	-4.00	-3.09	23.000	0.000	26.000	0.000
2	11	12	0.00	0.00	3.00	0.00	0.00	-4.00	-3.09	23.000	0.000	26.000	0.000
3	8	9	0.00	0.00	3.00	0.00	0.00	-4.00	-1.11	24.000	0.000	0.000	0.000
4	13	14	0.00	0.00	3.00	0.00	0.00	-4.00	-1.11	24.000	0.000	0.000	0.000

Function No. 1 Seat FDF NTI(1) = 1 Cards E

D0	D1	D2	D3	D4
0.0000	-3.0000	0.0000	0.0000	0.0000

First Part of Function - 4 Tabular Points

D	F(D)
0.000000	0.0000
1.000000	1000.0000
2.000000	2500.0000
3.000000	4500.0000

Function No. 2 Rear Board FDF NTI(2) = 15 Cards E

D0	D1	D2	D3	D4
0.0000	-2.0000	0.0000	0.0000	0.0000

First Part of Function - 3 Tabular Points

D	F(D)
0.000000	0.0000
1.000000	1000.0000
2.000000	2500.0000

Function No. 3 Floor FDF NTI(3) = 27 Cards E

D0	D1	D2	D3	D4
0.0000	-3.0000	0.0000	0.0000	0.0000

First Part of Function - 4 Tabular Points

D	F(D)
0.000000	0.0000
1.000000	1000.0000
2.000000	2500.0000

3.000000 4500.0000

Function No. 4 Belt Function NTI(4) = 41 Cards E

D0	D1	D2	D3	D4
0.0000	-3.0000	0.0000	0.0000	0.0000

First Part of Function - 4 Tabular Points

D	F(D)
0.000000	0.0000
0.050000	800.0000
0.100000	2000.0000
0.250000	4000.0000

Function No. 11 Head-FDF NTI(11) = 55 Cards E

D0	D1	D2	D3	D4
0.0000	-0.3500	0.0000	0.0000	0.0000

First Part of Function - 5 Tabular Points

D	F(D)
0.000000	0.0000
0.100000	500.0000
0.200000	1500.0000
0.300000	3500.0000
0.350000	5500.0000

Function No. 12 Face-FDF NTI(12) = 71 Cards E

D0	D1	D2	D3	D4
0.0000	-1.2500	0.0000	0.0000	0.0000

First Part of Function - 6 Tabular Points

D	F(D)
0.000000	0.0000

0.250000	250.0000
0.500000	500.0000
0.700000	1000.0000
0.900000	2000.0000
1.100000	3000.0000

1 Page 12

Function No. 13 Thorax-FDF NTI(13) = 89 Cards E

D0	D1	D2	D3	D4
0.0000	-3.5000	0.0000	0.0000	0.0000

First Part of Function - 5 Tabular Points

D	F(D)
0.000000	0.0000
1.500000	225.0000
2.500000	675.0000
3.500000	1125.0000
0.000000	0.0000

Function No. 14 UpAbd-FDF NTI(14) = 105 Cards E

D0	D1	D2	D3	D4
0.0000	-2.7500	0.0000	0.0000	0.0000

First Part of Function - 8 Tabular Points

D	F(D)
0.000000	0.0000
0.500000	200.0000
1.000000	400.0000
1.500000	600.0000
2.000000	1200.0000
2.250000	2400.0000
2.500000	3600.0000
2.750000	4800.0000

1 Page 13

Function No. 15 LoAbd-FDF NTI(15) = 127 Cards E

D0	D1	D2	D3	D4
0.0000	-3.5000	0.0000	0.0000	0.0000

First Part of Function - 9 Tabular Points

D	F(D)
0.000000	0.0000
0.500000	100.0000
1.000000	200.0000
1.500000	300.0000
2.000000	500.0000
2.500000	1000.0000
3.000000	2000.0000
3.250000	3000.0000
3.500000	5000.0000

Function No. 16 Knee-FDF NTI(16) = 151 Cards E

D0	D1	D2	D3	D4
0.0000	-0.2700	0.0000	0.0000	0.0000

First Part of Function - 5 Tabular Points

D	F(D)
0.000000	0.0000
0.100000	400.0000
0.200000	1200.0000
0.250000	2000.0000
0.270000	3000.0000

1

Function No. 17 PelvisBottom NTI(17) = 167 Cards E

D0	D1	D2	D3	D4
0.0000	-1.5000	0.0000	0.0000	0.0000

First Part of Function - 6 Tabular Points

D	F(D)
0.000000	0.0000
0.500000	38.0000
0.750000	64.0000
1.000000	110.0000
1.250000	240.0000
1.500000	760.0000

Function No. 18 PelvisBack NTI(18) = 185 Cards E

D0	D1	D2	D3	D4
0.0000	-1.0500	0.0000	0.0000	0.0000

First Part of Function - 5 Tabular Points

D	F(D)
0.000000	0.0000
0.500000	51.0000
0.750000	100.0000
1.000000	540.0000
1.050000	750.0000

Function No. 19 FemurFront NTI(19) = 201 Cards E

D0	D1	D2	D3	D4
0.0000	-1.5500	0.0000	0.0000	0.0000

First Part of Function - 6 Tabular Points

D	F(D)
0.000000	0.0000
0.500000	65.0000
1.000000	120.0000
1.250000	250.0000
1.500000	730.0000
1.550000	920.0000

Function No. 20 FemurBack NTI(20) = 219 Cards E

D0	D1	D2	D3	D4
0.0000	-2.1000	0.0000	0.0000	0.0000

First Part of Function - 7 Tabular Points

D	F(D)
0.000000	0.0000
0.500000	15.0000
1.000000	39.0000
1.500000	87.0000

1.750000	150.0000
2.000000	400.0000
2.100000	610.0000

1

Function No. 21 TibiaFront NTI(21) = 239 Cards E

D0	D1	D2	D3	D4
0.0000	-0.4500	0.0000	0.0000	0.0000

First Part of Function - 6 Tabular Points

D	F(D)
0.000000	0.0000
0.250000	2.0000
0.300000	6.0000
0.350000	49.0000
0.400000	140.0000
0.450000	250.0000

Function No. 22 TibiaBack NTI(22) = 257 Cards E

D0	D1	D2	D3	D4
0.0000	-0.5000	0.0000	0.0000	0.0000

First Part of Function - 6 Tabular Points

D	F(D)
0.000000	0.0000
0.200000	13.0000
0.300000	62.0000
0.400000	200.0000
0.450000	370.0000
0.500000	580.0000

1

Function No. 23 Femur Puck NTI(23) = 275 Cards E

D0	D1	D2	D3	D4
-1.0000	-1.0000	0.0000	0.0000	0.0000

First Part of Function - 7 Tabular Points

D	F(D)
-1.000000	-8300.0000

-0.800000	-4800.0000
-0.600000	-2900.0000
-0.400000	-1800.0000
-0.200000	-1100.0000
0.000000	0.0000
1.000000	4150.0000

Function No. 24 TibiaPuck NTI(24) = 295 Cards E

D0	D1	D2	D3	D4
-1.3000	-1.0000	0.0000	0.0000	0.0000

First Part of Function - 9 Tabular Points

D	F(D)
-1.300000	-3400.0000
-1.200000	-2700.0000
-1.000000	-1800.0000
-0.800000	-1250.0000
-0.600000	-900.0000
-0.400000	-700.0000
-0.200000	-350.0000
0.000000	0.0000
1.000000	1800.0000

1

Function No. 25 Foot-FDF NTI(25) = 319 Cards E

D0	D1	D2	D3	D4
0.0000	-1.2000	0.0000	0.0000	0.0000

First Part of Function - 7 Tabular Points

D	F(D)
0.000000	0.0000
0.200000	500.0000
0.400000	820.0000
0.600000	1380.0000
0.800000	2200.0000
1.000000	3800.0000
1.200000	6600.0000

Function No. 26 Damp-1.0 NTI(26) = 339 Cards E

D0	D1	D2	D3	D4
-500.0000	-500.0000	0.0000	0.0000	0.0000

First Part of Function - 3 Tabular Points

D	F(D)
-500.000000	-500.0000
0.000000	0.0000
500.000000	500.0000

1

Function No. 27 Damp-2.0 NTI(27) = 351 Cards E

D0	D1	D2	D3	D4
-500.0000	-500.0000	0.0000	0.0000	0.0000

First Part of Function - 3 Tabular Points

D	F(D)
-500.000000	-1000.0000
0.000000	0.0000
500.000000	1000.0000

Function No. 28 Head-Damp NTI(28) = 363 Cards E

D0	D1	D2	D3	D4
-500.0000	-500.0000	0.0000	0.0000	0.0000

First Part of Function - 3 Tabular Points

D	F(D)
-500.000000	-250.0000
0.000000	0.0000
500.000000	250.0000

1

Function No. 29 Face-Damp NTI(29) = 375 Cards E

D0	D1	D2	D3	D4
-100.0000	-100.0000	0.0000	0.0000	0.0000

First Part of Function - 3 Tabular Points

D	F(D)
-100.000000	-200.0000
0.000000	0.0000
100.000000	200.0000

Function No. 30 Thorax-Damp NTI(30) = 387 Cards E

D0	D1	D2	D3	D4
-500.0000	-100.0000	0.0000	0.0000	0.0000

First Part of Function - 4 Tabular Points

D	F(D)
-500.000000	-1200.0000
-100.000000	-240.0000
0.000000	0.0000
100.000000	300.0000

1

Function No. 31 LoAbd-Damp NTI(31) = 401 Cards E

D0	D1	D2	D3	D4
-500.0000	-500.0000	0.0000	0.0000	0.0000

First Part of Function - 3 Tabular Points

D	F(D)
-500.000000	-300.0000
0.000000	0.0000
500.000000	300.0000

Function No. 32 Knee-Damp NTI(32) = 413 Cards E

D0	D1	D2	D3	D4
-500.0000	-500.0000	0.0000	0.0000	0.0000

First Part of Function - 3 Tabular Points

D	F(D)
-500.000000	-750.0000
0.000000	0.0000
500.000000	750.0000

1 Page 22

Function No. 41 Low Fric (.25) NTI(41) = 425 Cards E

D0	D1	D2	D3	D4
0.0000	0.0000	0.2500	0.0000	0.0000

Function is Constant 0.250000

Function No. 42 Mid Fric (.5) NTI(42) = 430 Cards E

D0	D1	D2	D3	D4
0.0000	0.0000	0.5000	0.0000	0.0000

Function is Constant 0.500000

1 Page 23

Function No. 43 High Fric (.8) NTI(43) = 435 Cards E

D0	D1	D2	D3	D4
0.0000	0.0000	0.8000	0.0000	0.0000

Function is Constant 0.800000

Function No. 45 Belt Fric NTI(45) = 440 Cards E

D0	D1	D2	D3	D4
0.0000	0.0000	0.8000	0.0000	0.3000

Function is Constant 0.800000

1 Joint Force Function No. 81 LumbarJoint NTI(81) = 445 Page 24 Cards E.7

D0	D1	D2	D3	Ref. Segment
0.0000	0.0000	0.0000	0.0000	0.0000

0 Function is coefficients of 1 order polynomials in (THETA-THETA0) for 4 values of PHI.

PHI	THETA0	coefficients of (THETA-THETA0)**N N = 1
-180.00	0.000	2660.000
-90.00	0.000	7140.000
0.00	0.000	2660.000
90.00	0.000	7140.000

1 Joint Force Function No. 82 ThoracicJoint NTI(82) = 460

D0	D1	D2	D3	Ref. Segment
0.0000	0.0000	0.0000	0.0000	0.0000

0 Function is coefficients of 1 order polynomials in (THETA-THETA0) for 4 values of PHI.

PHI	THETA0	coefficients of (THETA-THETA0)**N N = 1
-180.00	0.000	4930.000
-90.00	0.000	21400.00
0.00	0.000	4930.000
90.00	0.000	21400.00

1 Joint Force Function No. 83 NeckPivot NTI(83) = 475

D0	D1	D2	D3	Ref. Segment
0.0000	0.0000	0.0000	0.0000	0.0000

0 Function is tabular for 10 X 4 values of THETA and PHI

PHI	THETA0	THETA 20.000	40.000	60.000	80.000	100.000
		120.000	140.000	160.000	180.000	
-180.00	0.000	800.0000	1400.000	2300.000	3900.000	6700.000
		11000.00	20000.00	33000.00	57000.00	
-90.00	0.000	750.0000	1000.000	2100.000	2800.000	3800.000
		5200.000	7000.000	9500.000	13000.00	
0.00	0.000	710.0000	989.9999	1400.000	2000.000	2700.000
		3800.000	5400.000	7600.000	11000.00	
90.00	0.000	750.0000	1000.000	2100.000	2800.000	3800.000
		5200.000	7000.000	9500.000	13000.00	

1 Joint Force Function No. 84 OCJoint NTI(84) = 522

D0	D1	D2	D3	Ref. Segment
0.0000	0.0000	0.0000	0.0000	0.0000

0 Function is tabular for 10 X 4 values of THETA and PHI

PHI	THETA0	THETA 20.000	40.000	60.000	80.000	100.000
		120.000	140.000	160.000	180.000	
-180.00	0.000	500.0000	1000.000	1400.000	2500.000	3200.000
		6000.000	10000.00	14000.00	20000.00	
-90.00	0.000	750.0000	1000.000	2100.000	2800.000	3800.000
		5200.000	7000.000	9500.000	13000.00	
0.00	0.000	400.0000	1000.000	1300.000	1800.000	2300.000
		2600.000	3600.000	5000.000	6800.000	
90.00	0.000	750.0000	1000.000	2100.000	2800.000	3800.000
		5200.000	7000.000	9500.000	13000.00	

1 Joint Force Function No. 85 Right Shoulder Joint NTI(85) = 569

D0	D1	D2	D3	Ref. Segment
0.0000	0.0000	0.0000	0.0000	0.0000

0 Function is coefficients of 2 order polynomials in (THETA-THETA0) for 4 values of PHI.

PHI	THETA0	coefficients of (THETA-THETA0)**N N = 1	N = 2
-180.00	165.000	-520.0000	5320.000
-90.00	0.000	150.0000	240.0000
0.00	30.000	0.000000	310.0000
90.00	115.000	210.0000	380.0000

1 Joint Force Function No. 86 Left Shoulder Joint NTI(86) = 588

D0	D1	D2	D3	Ref. Segment
0.0000	0.0000	0.0000	0.0000	0.0000

0 Function is coefficients of 2 order polynomials in (THETA-THETA0) for 4 values of PHI.

PHI	THETA0	coefficients of (THETA-THETA0)**N N = 1	N = 2
-180.00	165.000	-520.0000	5320.000
-90.00	30.000	0.000000	310.0000
0.00	115.000	210.0000	380.0000

90.00 0.000 150.0000 240.0000

1 Joint Force Function No. 87 Right Hip Joint NTI(87) = 607

D0	D1	D2	D3	Ref. Segment
0.0000	0.0000	0.0000	0.0000	0.0000

0 Function is tabular for 19 X 4 values of THETA and PHI

PHI	THETA0	THETA 10.000	20.000	30.000	40.000	50.000
		60.000	70.000	80.000	90.000	100.000
		110.000	120.000	130.000	140.000	150.000
		160.000	170.000	180.000		
-180.00	0.000	80.00000	180.0000	280.0000	390.0000	490.0000
		610.0000	720.0000	830.0000	950.0000	1100.000
		1200.000	1300.000	1400.000	1600.000	1700.000
		1800.000	2000.000	2100.000		
-90.00	0.000	130.0000	440.0000	930.0000	1600.000	2500.000
		3500.000	4800.000	6200.000	7800.000	9500.000
		12000.00	14000.00	16000.00	19000.00	21000.00
		24000.00	27000.00	30000.00		
0.00	0.000	150.0000	180.0000	230.0000	280.0000	350.0000
		430.0000	530.0000	660.0000	810.0001	1000.000
		1200.000	1500.000	1900.000	2400.000	2900.000
		3600.000	4500.000	5600.000		
90.00	0.000	50.00000	90.00000	540.0000	600.0000	790.0000
		1100.000	1500.000	2100.000	2800.000	3600.000
		4500.000	5500.000	6700.000	8000.000	9400.000
		11000.00	13000.00	14000.00		

1 Joint Force Function No. 88 Left Hip Joint NTI(88) = 690

D0	D1	D2	D3	Ref. Segment
0.0000	0.0000	0.0000	0.0000	0.0000

0 Function is tabular for 19 X 4 values of THETA and PHI

PHI	THETA0	THETA 10.000	20.000	30.000	40.000	50.000
		60.000	70.000	80.000	90.000	100.000
		110.000	120.000	130.000	140.000	150.000
		160.000	170.000	180.000		
-180.00	0.000	80.00000	180.0000	280.0000	390.0000	490.0000
		610.0000	720.0000	830.0000	950.0000	1100.000
		1200.000	1300.000	1400.000	1600.000	1700.000
		1800.000	2000.000	2100.000		

-90.00	0.000	50.00000	90.00000	540.0000	600.0000	790.0000
		1100.000	1500.000	2100.000	2800.000	3600.000
		4500.000	5500.000	6700.000	8000.000	9400.000
		11000.00	13000.00	14000.00		
0.00	0.000	150.0000	180.0000	230.0000	280.0000	350.0000
		430.0000	530.0000	660.0000	810.0001	1000.000
		1200.000	1500.000	1900.000	2400.000	2900.000
		3600.000	4500.000	5600.000		
90.00	0.000	130.0000	440.0000	930.0000	1600.000	2500.000
		3500.000	4800.000	6200.000	7800.000	9500.000
		12000.00	14000.00	16000.00	19000.00	21000.00
		24000.00	27000.00	30000.00		

1 Joint Force Function No. 89 Ankle Flexion NTI(89) = 773 Page 32
Cards E.7

D0	D1	D2	D3	Ref. Segment
0.0000	0.0000	0.0000	0.0000	0.0000

0 Function is tabular for 10 X 4 values of THETA and PHI

		THETA				
PHI	THETA0	20.000	40.000	60.000	80.000	100.000
		120.000	140.000	160.000	180.000	
-180.00	0.000	0.000000	0.000000	350.0000	830.0000	1530.000
		2440.000	3570.000	4920.000	6480.000	
-90.00	0.000	40.00000	340.0000	920.0000	1760.000	2880.000
		4260.000	5920.000	7840.000	10000.00	
0.00	0.000	220.0000	839.9999	1860.000	3270.000	5090.000
		7300.000	9910.000	12900.00	16300.00	
90.00	0.000	40.00000	340.0000	920.0000	1760.000	2880.000
		4260.000	5920.000	7840.000	10000.00	

1 Joint Force Function No. 90 Ankle Torsion NTI(90) = 820 Page 33
Cards E.7

D0	D1	D2	D3	Ref. Segment
0.0000	0.0000	0.0000	0.0000	0.0000

0 Function is tabular for 10 X 2 values of THETA and PHI

		THETA				
PHI	THETA0	20.000	40.000	60.000	80.000	100.000
		120.000	140.000	160.000	180.000	
-180.00	0.000	160.0000	2370.000	9100.000	19500.00	33600.00
		51400.00	72900.00	98099.98	127000.0	
0.00	0.000	160.0000	2370.000	9100.000	19500.00	33600.00
		51400.00	72900.00	98099.98	127000.0	

1 Allowed Contacts and Associated Functions Page 34

```
0                                                                                                                    Cards F.1
0     Plane          Segment  Force Deflection      Inertial Spike     R Factor        G Factor     Friction Coef. Opt     Output
0      1- 22          1- 1       1                0                  0                  0               42           1           0
 seat                  pelv Seat FDF                                                                                  Mid Fric (.5)
0      1- 22          6- 6       1                0                  0                  0               42           1           0
 seat                  rulu Seat FDF                                                                                  Mid Fric (.5)
0      1- 22          7- 7       1                0                  0                  0               42           1           0
 seat                  rull Seat FDF                                                                                  Mid Fric (.5)
0      1- 22         11- 11      1                0                  0                  0               42           1           0
 seat                  lulu Seat FDF                                                                                  Mid Fric (.5)
0      1- 22         12- 12      1                0                  0                  0               42           1           0
 seat                  lull Seat FDF                                                                                  Mid Fric (.5)
0      2- 22          1- 1       2                0                  0                  0               42           1           0
 seat                  pelv Rear Board FDF                                                                            Mid Fric (.5)
0      2- 22          2- 2       2                0                  0                  0               42           1           0
 seat                  lthx Rear Board FDF                                                                            Mid Fric (.5)
0      2- 22          3- 3       2                0                  0                  0               42           1           0
 seat                  uthx Rear Board FDF                                                                            Mid Fric (.5)
0      2- 22          4- 4       2                0                  0                  0               42           1           0
 seat                  nk   Rear Board FDF                                                                            Mid Fric (.5)
0      2- 22          5- 5       2                0                  0                  0               42           1           0
 seat                  hd   Rear Board FDF                                                                            Mid Fric (.5)
0      3- 22         10- 10      3                0                  0                  0               43          -1           0
 floor                 rf   Floor FDF                                                                                 High Fric (.8)
0      3- 22         15- 15      3                0                  0                  0               43          -1           0
 floor                 lf   Floor FDF                                                                                 High Fric (.8)
0      3- 22          5- 23      3                0                  0                  0               43          -1           0
 floor                 hd   Floor FDF                                                                                 High Fric (.8)
0      3- 22          3- 24      3                0                  0                  0               43           0           0
 floor                 uthx Floor FDF                                                                                High Fric (.8)
0                                                                                                                    Cards F.3
0     Segment         Segment  Force Deflection      Inertial Spike     R Factor        G Factor     Friction Coef. Opt     Output
0       6- 6          11- 11     19               0                  0                  0               42           0
          rulu         lulu FemurFront                                                                                Mid Fric (.5)
0       7- 7          12- 12     19               0                  0                  0               42           0
          rull         lull FemurFront                                                                                Mid Fric (.5)
1 Harness-Belt System Input                                                                                            Page   35
                                                                                                                     Cards F.8

  No. of Harnesses =   1

  No. of Belts per Harness =     2     0     0     0     0          MAXITR =  10     EPSDEL = 0.01000
0 For Harness No.  1 No. of Points per Belt =   6   7
0 Harness No.  1 Belt No.  1 Function Nos.     4     0     0     0     0  Reference Slack =     0.000 IN

0    K    KS    KE    NT    NPD   NDR    Function Nos.                                                              Cards F.8.D

     1    22     0   103     1     1     0     0     0     0     0
     2     3    24   115     0     0     0     0     0     0     0
     3     3     3   127     0     0     0     0     0     0     0
     4     3     3   139     0     0     0     0     0     0     0
     5     2     2   151     0     0     0     0     0     0     0
```

6	2	2	163	0	0	0	0	0	0	0
7	1	1	175	0	0	0	0	0	0	0
8	22	0	187	1	1	0	0	0	0	0

0

	Base Reference (IN)			Adjusted Reference (IN)			Offset (IN)			Preferred Direction (IN)		
K	X	Y	Z	X	Y	Z	X	Y	Z	X	Y	Z
1	-47.466	-7.826	-33.470	-47.466	-7.826	-33.470	0.000	0.000	0.000	0.000	0.000	-1.000
2	2.111	-2.709	-1.158	1.779	-2.282	-0.975	0.000	0.000	-1.500	0.000	0.000	0.000
3	3.750	-1.376	-1.054	4.162	-1.527	-1.170	0.600	0.000	1.450	0.000	0.000	0.000
4	3.608	0.094	1.372	4.205	0.109	1.599	0.600	0.000	1.450	0.000	0.000	0.000
5	1.675	2.462	-0.650	3.127	4.595	-1.214	0.450	0.000	-2.400	0.000	0.000	0.000
6	1.088	3.278	1.540	1.648	4.963	2.331	0.450	0.000	-2.400	0.000	0.000	0.000
7	-0.981	4.993	-1.506	-1.269	6.456	-1.947	0.500	0.000	-0.750	0.000	0.000	0.000
8	-32.491	9.402	-0.597	-32.491	9.402	-0.597	0.000	0.000	0.000	0.000	0.000	-1.000

0 Harness No. 1 Belt No. 2 Function Nos. 4 0 0 0 0 Reference Slack = 0.000 IN

0

K	KS	KE	NT	NPD	NDR	Function Nos.					Cards F.8.D
9	22	0	199	1	1	0	0	0	0	0	
10	1	1	211	0	0	0	0	0	0	0	
11	1	1	223	0	0	0	0	0	0	0	
12	1	1	235	0	0	0	0	0	0	0	
13	1	1	247	0	0	0	0	0	0	0	
14	1	1	259	0	0	0	0	0	0	0	
15	22	0	271	1	1	0	0	0	0	0	

0

	Base Reference (IN)			Adjusted Reference (IN)			Offset (IN)			Preferred Direction (IN)		
K	X	Y	Z	X	Y	Z	X	Y	Z	X	Y	Z
9	-32.327	-9.726	-1.085	-32.327	-9.726	-1.085	0.000	0.000	0.000	0.000	0.000	-1.000
10	2.354	-6.600	1.350	2.237	-6.272	1.283	0.500	0.000	-0.750	0.000	0.000	0.000
11	4.030	-3.300	-0.850	4.436	-3.632	-0.935	0.500	0.000	-0.750	0.000	0.000	0.000
12	4.762	0.000	-1.733	4.934	0.000	-1.795	0.500	0.000	-0.750	0.000	0.000	0.000
13	4.030	3.300	-0.850	4.435	3.632	-0.936	0.500	0.000	-0.750	0.000	0.000	0.000
14	2.354	6.600	1.350	2.237	6.272	1.283	0.500	0.000	-0.750	0.000	0.000	0.000
15	-32.327	9.565	-1.164	-32.327	9.565	-1.164	0.000	0.000	0.000	0.000	0.000	-1.000

1 Subroutine INPUT_INITIAL Input I1 = 0, J1 = 0, I3 = 0 Page 36

Card G.1

0 Initial Positions

Segment	Linear Position (IN) (IREF4 Reference)			Linear Velocity (IN /SEC) (Inertial)				Cards G.2
No. Seg	X	Y	Z	X	Y	Z	IREF2	IREF4
1 pelv	-30.64789	-0.00001	-11.14996	0.00000	0.00000	0.00000	0	0
2 lthx	-32.95438	-0.00001	-17.68664	0.00000	0.00000	0.00000	0	0
3 uthx	-37.19260	-0.00001	-26.97534	0.00000	0.00000	0.00000	0	0
4 nk	-38.61640	-0.00001	-31.98280	0.00000	0.00000	0.00000	0	0
5 hd	-37.87640	-0.00001	-36.57280	0.00000	0.00000	0.00000	0	0
6 rulu	-26.05311	4.48999	-11.14402	0.00000	0.00000	0.00000	0	0
7 rull	-16.47239	4.78999	-14.20545	0.00000	0.00000	0.00000	0	0
8 rllu	-10.82044	4.83999	-12.71110	0.00000	0.00000	0.00000	0	0
9 rlll	-4.67976	4.68999	-7.42792	0.00000	0.00000	0.00000	0	0

10 rf	0.80276	4.83999	-4.39402	0.00000	0.00000	0.00000	0	0
11 lulu	-26.05311	-4.49001	-11.14402	0.00000	0.00000	0.00000	0	0
12 lull	-16.47239	-4.79001	-14.20545	0.00000	0.00000	0.00000	0	0
13 lllu	-10.82044	-4.84001	-12.71110	0.00000	0.00000	0.00000	0	0
14 llll	-4.67976	-4.69001	-7.42792	0.00000	0.00000	0.00000	0	0
15 lf	0.80276	-4.84001	-4.39402	0.00000	0.00000	0.00000	0	0
16 rua	-36.71016	7.37999	-24.19075	0.00000	0.00000	0.00000	0	0
17 rla	-31.81104	7.37999	-17.35456	0.00000	0.00000	0.00000	0	0
18 rhd	-25.33664	7.37999	-12.31351	0.00000	0.00000	0.00000	0	0
19 lua	-36.71016	-7.38001	-24.19075	0.00000	0.00000	0.00000	0	0
20 lla	-31.81104	-7.38001	-17.35456	0.00000	0.00000	0.00000	0	0
21 lhd	-25.33664	-7.38001	-12.31351	0.00000	0.00000	0.00000	0	0

0 Initial Angular Rotation and Velocity

Cards G.3

Segment	Angular Rotation (deg) (IYPR4 Reference)			Angular Velocity (deg/SEC) (Local)			IYPR			
No. Seg	Yaw	Pitch	Roll	X	Y	Z				
1 pelv	0.00000	15.00000	0.00000	0.00000	0.00000	0.00000	1	2	3	23
2 lthx	0.00000	22.00000	0.00000	0.00000	0.00000	0.00000	1	2	3	23
3 uthx	0.00000	22.00000	0.00000	0.00000	0.00000	0.00000	1	2	3	23
4 nk	0.00000	0.00000	0.00000	0.00000	0.00000	0.00000	1	2	3	23
5 hd	0.00000	0.00000	0.00000	0.00000	0.00000	0.00000	1	2	3	23
6 rulu	0.00000	110.00000	0.00000	0.00000	0.00000	0.00000	1	2	3	23
7 rull	0.00000	110.00000	0.00000	0.00000	0.00000	0.00000	1	2	3	23
8 rllu	0.00000	50.00000	0.00000	0.00000	0.00000	0.00000	1	2	3	23
9 rlll	0.00000	50.00000	0.00000	0.00000	0.00000	0.00000	1	2	3	23
10 rf	0.00000	50.00000	0.00000	0.00000	0.00000	0.00000	1	2	3	23
11 lulu	0.00000	110.00000	0.00000	0.00000	0.00000	0.00000	1	2	3	23
12 lull	0.00000	110.00000	0.00000	0.00000	0.00000	0.00000	1	2	3	23
13 lllu	0.00000	50.00000	0.00000	0.00000	0.00000	0.00000	1	2	3	23
14 llll	0.00000	50.00000	0.00000	0.00000	0.00000	0.00000	1	2	3	23
15 lf	0.00000	50.00000	0.00000	0.00000	0.00000	0.00000	1	2	3	23
16 rua	0.00000	25.00000	0.00000	0.00000	0.00000	0.00000	1	2	3	23
17 rla	0.00000	50.00000	0.00000	0.00000	0.00000	0.00000	1	2	3	23
18 rhd	0.00000	50.00000	0.00000	0.00000	0.00000	0.00000	1	2	3	23
19 lua	0.00000	25.00000	0.00000	0.00000	0.00000	0.00000	1	2	3	23
20 lla	0.00000	50.00000	0.00000	0.00000	0.00000	0.00000	1	2	3	23
21 lhd	0.00000	50.00000	0.00000	0.00000	0.00000	0.00000	1	2	3	23

0 Linear and angular velocities have been set equal to the initial velocities of the primary vehicle for all nonvehicle body segments with IREF2 = 0. For nonvehicle segments with IREF2 # 0, the linear and angular velocities were determined by the values of IREF2.

```
0 HBPLAY Time =     0.000 msec. NH,NB,NPTS NT=     1     1     7    97
  NL(1)=       1       2       3       4       5       7       8
  BB   =      12.810   4.131   3.217   5.765   9.081  13.296
0 HBPLAY Time =     0.000 msec. NH,NB,NPTS NT=     1     2     7   193
  NL(1)=       9      10      11      12      13      14      15
  BB   =      11.708   4.089   3.765   3.765   4.089  11.592
```

Tabular Time History Control Parameters

Type KSG Selected Segments or Joints

```
H. 1   3      5  6  7
   Ref        0  0  0
H. 2   1      5
   Ref        0
H. 3   2      5  7
   Ref        0  6
H. 4   0
   Ref
H. 5   0
   Ref
H. 6   0
   Ref
H. 7   0
H. 8   0
   Ref
H. 9   0
```